Am J Cancer Res 2026;16(10):4254-4277
www.ajcr.us /ISSN:2156-6976/ajcr0173372

Original Article

Combination of the modified 5-item frailty index and novel platelet index score for predicting long-term prognosis in hepatocellular carcinoma patients treated with transarterial chemoembolization

Chengbo Tang[1*], Ziying Deng[2*], Jia Liu[3], Hao Zhang[4], Feng Guo[1], Xun Ma[2]

[1]Department of Interventional Diagnosis and Treatment, Yongzhou Central Hospital, Yongzhou Clinical College, University of South China, Yongzhou 425000, Hunan, China; [2]Department of Oncology, Yongzhou Central Hospital, Yongzhou Clinical College, University of South China, Yongzhou 425000, Hunan, China; [3]Department of Oncology, The First Peoples' Hospital of Changde City, 818 Renmin Road, Wuling District, Changde 415003, Hunan, China; [4]Department of Interventional Vascular Surgery, First Affiliated Hospital of Hunan Normal University (Hunan Provincial People's Hospital), Changsha 410000, Hunan, China. [*]Equal contributors.

Received April 16, 2026; Accepted September 1, 2026; Epub October 15, 2026; Published October 30, 2026

Abstract: Hepatocellular carcinoma (HCC) is one of the leading causes of cancer-related deaths worldwide. Transcatheter arterial chemoembolization (TACE) represents an important treatment modality for unresectable HCC; however, marked heterogeneity exists in long-term survival and progression-free survival among patients, underscoring the need for effective predictive tools. This study aimed to evaluate the value of a combined index incorporating the 5-factor modified Frailty Index (mFI-5) and the novel platelet index score (PIS) in predicting overall survival (OS) and progression-free survival (PFS) in HCC patients undergoing TACE. A total of 237 HCC patients who received TACE between March 2018 and March 2023 were enrolled and randomly divided into a training cohort (n = 168) and an internal validation cohort (n = 69) in a 7:3 ratio. An additional 105 HCC patients treated with TACE at the First People's Hospital of Changde between January 2019 and December 2022 were included as an external validation cohort. A combined mFI-5+PIS score was constructed, and its predictive performance was assessed using Cox proportional hazards regression, Kaplan-Meier survival analysis, time-dependent receiver operating characteristic (ROC) curves, and nomogram models. Higher mFI-5+PIS scores were significantly associated with shorter OS and PFS (Log-rank P < 0.001). Multivariable analysis confirmed that mFI-5+PIS was an independent predictor of both OS (HR = 1.8, 95% CI: 1.4-2.4, P < 0.001) and PFS (HR = 2.2, 95% CI: 1.6-3.1, P < 0.001). Subgroup analyses demonstrated that the mFI-5+PIS score consistently stratified patients into high- and low-risk groups across diverse etiologies (HBV, HCV, and others), treatment regimens (TACE alone versus TACE combined with targeted therapy and immunotherapy), portal vein tumor thrombus (PVTT) status, and tumor size categories (all subgroup Log-rank P < 0.05). Interaction tests further revealed that PVTT (P_interaction = 0.061 for OS; 0.143 for PFS) and tumor size (P_interaction = 0.166 for OS; 0.305 for PFS) did not significantly modify the prognostic effect of the score, suggesting that the score's risk stratification is independent of these key clinical factors. The nomogram based on the combined score exhibited excellent predictive performance, with concordance indices (C-index) of 0.795 for OS and 0.821 for PFS. The independent prognostic value of the combined score was consistently validated in both internal and external cohorts, and the corresponding nomogram demonstrated good discrimination and calibration, confirming the model's generalizability. In conclusion, the mFI-5+PIS score is an independent predictor of OS and PFS in HCC patients receiving TACE, and the nomogram derived from this score demonstrates robust predictive performance, effectively identifying high-risk patients and facilitating individualized treatment decisions and prognostic management in clinical practice.

Keywords: Hepatocellular carcinoma, transarterial chemoembolization, modified 5-item frailty index, platelet index score, prognosis, nomogram

https://doi.org/10.62347/XHVB2260

Introduction

Hepatocellular carcinoma (HCC) is one of the most common malignant tumors in the world, with high incidence and mortality [1]. So far, the global incidence and mortality rates of HCC have continued to rise [2]. Surgical resection is still the preferred radical treatment plan for HCC; however, due to factors such as tumor size, location, stage, liver function, and vascular invasion, many patients do not have the indication for surgical resection; therefore, local treatment methods such as transarterial chemoembolization (TACE) have been introduced into clinical practice [3, 4]. TACE can not only effectively control the progression of tumors, but also be used as a translational treatment plan to downstage initially unresectable tumors, thus creating opportunities for surgical resection and significantly improving the long-term survival prognosis of patients [5]. The prognosis of patients with HCC is affected by many factors, such as demographic characteristics, tumor heterogeneity and clinical characteristics, which means that even if they receive TACE treatment, there are significant differences in the prognosis of patients [6, 7]. Therefore, identifying reliable biomarkers or evaluation tools that can accurately predict the efficacy and long-term prognosis of TACE is of great significance to guide individualized treatment and optimize clinical decision-making.

Frailty is a clinical syndrome reflecting an age-related decline in physiological reserve and increased susceptibility to stressors. It has been shown to effectively predict the risk of complications, death and long-term prognosis of elderly patients after surgery and interventional treatment [8]. Among various evaluation tools, the mFI-5, derived from the American College of Surgeons National Surgical Quality Improvement Program (ACS NSQIP) database, has been widely used to evaluate the prognosis of patients with various cancers, including liver, gastric, and brain tumors, demonstrating good performance [9-12]. The index contains 5 comorbidity dimensions, specifically functional status, diabetes, chronic obstructive pulmonary disease (COPD) or recent history of pneumonia, congestive heart failure, and hypertension requiring drug treatment, which can effectively evaluate the overall physiological vulnerability of patients [9].

Changes in platelet-related parameters are associated with the prognosis of various malignancies [13]. The novel platelet index score (PIS) is a comprehensive evaluation index that integrates the changes in platelet count (PLT), mean platelet volume (MPV) and platelet distribution width (PDW). A study on endometrial cancer confirmed that PIS has independent prognostic predictive value, and individualized risk stratification can be achieved through the nomogram [14]. This indicates that PIS derived from routine blood tests may be used as an economical, effective and widely applicable tumor prognostic biomarker. However, the application value of this score in the population of patients with HCC treated with TACE has not been fully explored.

The improved 5-item frailty index (mFI-5) and PIS have been proven to have prognostic evaluation value for different groups of malignant tumor patients. However, there is no specific study to apply these two indicators together to predict the long-term prognosis of patients with HCC treated with TACE. This study aims to explore the combined application of the above two indicators to predict OS and risk of disease progression after patients receive TACE treatment, and then assist clinicians in formulating more accurate treatment strategies.

Materials and methods

Study design and patient population

This retrospective study enrolled HCC patients who received their first TACE treatment at the Yongzhou Central Hospital between March 2018 and March 2023, and at the First People's Hospital of Changde City between January 2019 and December 2022. The inclusion criteria were as follows: (1) clinically confirmed diagnosis of HCC; (2) age ≥ 18 years; (3) receipt of TACE; and (4) complete clinical and follow-up data. The exclusion criteria included: (1) presence of other malignancies or non-primary liver cancer; (2) first follow-up time of less than 3 months (unless an event occurred within 3 months); (3) Child-Pugh class C; and (4) Eastern Cooperative Oncology Group performance status (ECOG PS) > 2. The study protocol was approved by the ethics committees of Yongzhou Central Hospital and the First People's Hospital of Changde City.

Data collection and endpoint definitions

We collected baseline data for all patients, including sex, age, BMI, ECOG PS score, portal vein tumor thrombus (PVTT), Barcelona Clinic Liver Cancer (BCLC) stage, tumor size, tumor number, etiology (hepatitis B virus, hepatitis C virus, etc.), Child-Pugh class, liver cirrhosis, ascites, laboratory parameters (alpha-fetoprotein [AFP], platelet parameters, total bilirubin [TB], albumin, etc.), mFI-5-related comorbidities (hypertension, diabetes mellitus, COPD/recent pneumonia, dependent functional status, and congestive heart failure), and treatment regimens (TACE alone or TACE combined with targeted therapy and immunotherapy).

OS is defined as the interval from the first TACE treatment to death for any cause or the last follow-up date. Progression-free survival (PFS) is defined by reference to the revised standard for the efficacy evaluation of solid tumors (mRECIST), that is, the time interval from the first TACE treatment to the first observation of imaging progression, death for any reason or the last follow-up date, subject to the first of the three events [15]. The last follow-up date of this study was June 2025.

Definitions of PIS and mFI-5

PIS was calculated based on the results of the routine blood test completed by venous blood collected within 1 week before the treatment of TACE. The detection of PLT, MPV and PDW was performed using the Meirui BC-6800 fully automatic blood cell analyzer. In the training center, the optimal cut-off values for PLT, MPV and PDW were determined using ROC curve analysis and the Youden index method, and then PIS was constructed based on the above cut-off values. The scoring criteria were as follows: 0 points for no abnormal indicators; 1 point for one abnormal indicator; 2 points for two abnormal indicators; and 3 points for three abnormal indicators.

The improved version of mFI-5 contains 5 evaluation items (1 point per item), specifically: COPD/recent pneumonia, diabetes, congestive heart failure, hypertension requiring drug treatment and dependent functional status. The total score of the index ranges from 0 to 5 points. Patients with an mFI-5 score of ≥ 2 were defined as 'frail', and those with a score of < 2 as 'non-frail'. The above scoring results are independently reviewed and confirmed by two doctors.

Statistical analysis

This study uses SPSS 26.0 statistical software (IBM, Armonk, New York, USA) and R software (version 4.5.1) to complete statistical analysis. Continuous variables conforming to the normal distribution are expressed as mean ± standard deviation ($\bar{x} \pm s$), and independent sample t test is used for intergroup comparison; continuous variables that do not conform to normal distribution are expressed as median (interquartile range) [M (IQR)], and Mann-Whitney U test is used for inter-group comparison. Categorical variables are expressed as numbers (percentages) [n (%)], and intergroup comparisons were performed using the chi-square test, Kruskal-Wallis H test, or Fisher's exact test, as appropriate. ROC curve analysis was used to determine the optimal cut-off values of PLT, MPV and PDW, and the area under the curve (AUC) and the Youden index (sensitivity + specificity - 1) were calculated. The survival curve is drawn by the Kaplan-Meier method for survival analysis, and Log-rank test is used for the comparison of survival differences between groups. Univariate and multivariate Cox proportional hazards regression models are used to screen independent risk factors affecting OS and PFS. The predictive efficiency of the nomogram is verified by the concordance index (C-index), calibration curve and time-dependent ROC curve: the closer C-index is to 1, the better the discrimination efficiency of the model; the closer the calibration curve is to the diagonal, the higher the calibration of the model. In this study, a two-sided P value < 0.05 was considered statistically significant. We used Cox proportional hazards models with product interaction terms to examine the interaction between the mFI-5+PIS score and key clinical stratification factors to determine whether the prognostic effect of the score was consistent across subgroups. An interaction P value < 0.05 was considered to indicate effect modification.

Results

Baseline patient characteristics

Following application of the inclusion and exclusion criteria, a total of 342 patients were ulti-

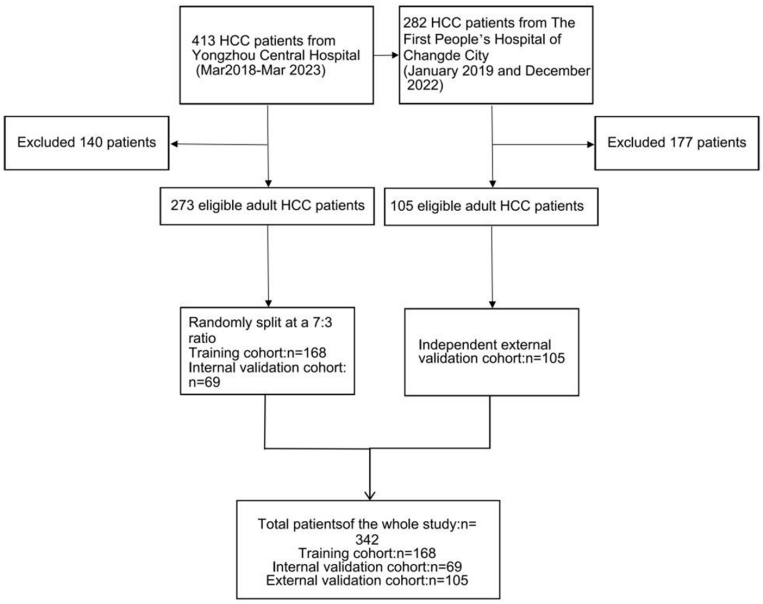

Figure 1. Flow chart of sample selection. HCC, Hepatocellular carcinoma; TACE, Transarterial chemoembolization; ECOG PS, Eastern Cooperative Oncology Group Performance Status; Child-Pugh, Child-Pugh classification for liver function.

mately enrolled. Among them, 237 patients from Yongzhou Central Hospital were randomly assigned to a training cohort (n = 168) and an internal validation cohort (n = 69) in a 7:3 ratio. The remaining 105 patients from the First People's Hospital of Changde City were all assigned to the external validation cohort (**Figure 1**). The overall cohort was predominantly male (270 patients, 78.9%) and had hepatitis B virus (HBV) infection (241 patients, 70.5%). Cirrhosis was present in 262 patients (76.6%), and 141 patients (41.2%) had portal vein tumor thrombus. The tumor burden was relatively high. Notably, 83.9% of patients were Child-Pugh class A, and 92.7% had an Eastern Cooperative Oncology Group performance status of 0 to 1 (**Table 1**).

mFI-5+PIS and prognostic stratification

Based on the area under the ROC curve (AUC) and the Youden index in the training set, the optimal cut off values for platelet parameters were determined. The diagnostic performance for each indicator at the corresponding cut off was as follows: for PLT, the cut off value was 108.55×10^9/L, yielding a sensitivity of 0.782, a specificity of 0.867, and a Youden index of 0.649. For MPV, the cut off was 10.65 fL, with a sensitivity of 0.758, a specificity of 0.889, and a Youden index of 0.647. For PDW, the cut off was 12.35 fL, resulting in a sensitivity of 0.742, a specificity of 0.800, and a Youden index of 0.542. Consequently, PLT ≤ 108.55×10^9/L, MPV ≥ 10.65 fL, and PDW ≥ 12.35 fL were selected as the cut offs for dichotomization. Internal validation was performed using 1000 bootstrap resampling. The median bootstrap cut offs for the three indicators were identical to the original cut offs. The median bootstrap sensitivity values for PLT, MPV, and PDW were 0.782, 0.774, and 0.758, respectively; the median bootstrap specificity values were 0.867, 0.889, and 0.800, respectively; the median bootstrap Youden indices were 0.656, 0.658, and 0.555; and the median bootstrap AUC values were 0.797, 0.852, and 0.785, respectively. These findings confirmed the stability and reliability of the cut offs and their diagnostic performance. ROC curve analysis demonstrated that all three platelet indicators had good predictive performance for OS, with MPV showing the best discriminative ability (AUC = 0.851; PLT AUC = 0.794; PDW AUC = 0.782) (**Figure 2**). Analysis of the associations between these three platelet indicators and clinical characteristics revealed that low PLT, high MPV, and high PDW were each significantly associated with poorer liver function (Child-Pugh class B), higher tumor burden (presence of portal vein tumor thrombus, maximum tumor diameter ≥ 5 cm, and multiple tumor nodules), and higher AFP level (≥ 200 μg/L) (all $P < 0.05$) (**Table 2**). Kaplan-Meier curves showed that low PLT, high MPV, and high PDW were associated with shorter OS and PFS (Log-rank $P < 0.001$) (**Figures 3A-C**, **4A-C**).

Based on the cut off values of the above platelet indicators, the PIS score was constructed. In the training set, the distribution of the PIS score was as follows: 53 patients (31.5%) scored 0, 17 (10.1%) scored 1, 11 (6.5%) scored 2, and 87 (51.8%) scored 3. Analysis of the

Table 1. Baseline characteristics of patients

Characteristic	Total (n = 342)	Training Cohort (n = 168)	Internal Validation cohort (n = 69)	External Validation cohort (n = 105)	Statistic (χ^2/t/U/H)	*P* Value
Sex					0.426	0.808
Female	72 (21.1)	33 (19.6)	15 (21.7)	24 (22.9)		
Male	270 (78.9)	135 (80.4)	54 (78.3)	81 (77.1)		
Age (years)					0.747	0.688
≥ 60	158 (46.2)	81 (48.2)	32 (46.4)	45 (42.9)		
< 60	184 (53.8)	87 (51.8)	37 (53.6)	60 (57.1)		
BMI (kg/m^2)					1.908	0.385
< 25	275 (80.4)	137 (81.5)	58 (84.1)	80 (76.2)		
≥ 25	67 (19.6)	31 (18.5)	11 (15.9)	25 (23.8)		
ECOG PS Score					0.354	0.838
0	110 (32.2)	51 (30.4)	23 (33.3)	36 (34.3)		
1	207 (60.5)	106 (63.1)	39 (56.5)	62 (59.0)		
2	25 (7.3)	11 (6.5)	7 (10.1)	7 (6.7)		
Child-Pugh					1.412	0.494
A	287 (83.9)	145 (86.3)	56 (81.2)	86 (81.9)		
B	55 (16.1)	23 (13.7)	13 (18.8)	19 (18.1)		
Hypertension					0.182	0.913
No	259 (75.7)	128 (76.2)	53 (76.8)	78 (74.3)		
Yes	83 (24.3)	40 (23.8)	16 (23.2)	27 (25.7)		
Diabetes Mellitus					5.833	0.054
No	251 (73.4)	129 (76.8)	54 (78.3)	68 (64.8)		
Yes	91 (26.6)	39 (23.2)	15 (21.7)	37 (35.2)		
COPD/Recent Pneumonia					8.043	0.018
No	269 (78.7)	141 (83.9)	55 (79.7)	73 (69.5)		
Yes	73 (21.3)	27 (16.1)	14 (20.3)	32 (30.5)		
Non-independent Functional Status					1.512	0.47
No	295 (86.3)	147 (87.5)	61 (88.4)	87 (82.9)		
Yes	47 (13.7)	21 (12.5)	8 (11.6)	18 (17.1)		
Congestive Heart Failure					1.433	0.489
No	319 (93.3)	154 (91.7)	65 (94.2)	100 (95.2)		
Yes	23 (6.7)	14 (8.3)	4 (5.8)	5 (4.8)		
PVTT					0.546	0.761
No	201 (58.8)	96 (57.1)	43 (62.3)	62 (59.0)		
Yes	141 (41.2)	72 (42.9)	26 (37.7)	43 (41.0)		
BCLC					0.005	0.997
A	38 (11.1)	16 (9.5)	7 (10.1)	15 (14.3)		
B	184 (53.8)	95 (56.5)	38 (55.1)	51 (48.6)		
C	120 (35.1)	57 (33.9)	24 (34.8)	39 (37.1)		
Maximum Tumor Diameter					1.012	0.603
< 5 cm	247 (72.2)	125 (74.4)	47 (68.1)	75 (71.4)		
≥ 5 cm	95 (27.8)	43 (25.6)	22 (31.9)	30 (28.6)		
Number of Tumors					2.912	0.233
Single	118 (34.5)	52 (31.0)	23 (33.3)	43 (41.0)		
Multiple	224 (65.5)	116 (69.0)	46 (66.7)	62 (59.0)		
Cause of disease					1.7	0.791
Hepatitis B Virus	241 (70.5)	122 (72.6)	46 (66.7)	73 (69.5)		
Hepatitis C Virus	35 (10.2)	15 (8.9)	7 (10.1)	13 (12.4)		
Others	66 (19.3)	31 (18.5)	16 (23.2)	19 (18.1)		

Cirrhosis					1.429	0.489
No	80 (23.4)	39 (23.2)	13 (18.8)	28 (26.7)		
Yes	262 (76.6)	129 (76.8)	56 (81.2)	77 (73.3)		
Ascites					0.246	0.884
No	256 (74.9)	124 (73.8)	53 (76.8)	79 (75.2)		
Yes	86 (25.1)	44 (26.2)	16 (23.2)	26 (24.8)		
AFP (ug/L)					1.344	0.511
< 200	119 (34.8)	60 (35.7)	20 (29.0)	39 (37.1)		
≥ 200	223 (65.2)	108 (64.3)	49 (71.0)	66 (62.9)		
TB (μmol/L)					4.129	0.127
≤ 17	89 (26.0)	36 (21.4)	19 (27.5)	34 (32.4)		
> 17	253 (74.0)	132 (78.6)	50 (72.5)	71 (67.6)		
Albumin (g/L)					1.697	0.428
≤ 35	248 (72.5)	127 (75.6)	49 (71.0)	72 (68.6)		
> 35	94 (27.5)	41 (24.4)	20 (29.0)	33 (31.4)		
PLT (×10^9/L)		96.81±36.10	97.12±36.49		0.06	0.952
MPV (fL)		11.04±1.54	11.00±1.62		0.173	0.863
PDW (fL)		12.74±1.45	12.62±1.46		0.582	0.561
mFI-5					0.114	0.945
< 2	209 (61.1)	103 (61.3)	41 (59.4)	65 (61.9)		
≥ 2	133 (38.9)	65 (38.7)	28 (40.6)	40 (38.1)		
Treatment					0.965	0.617
TACE		121 (72.0)	47 (68.1)	70 (66.7)		
TACE + targeted therapy and immunotherapy		47 (28.0)	22 (31.9)	35 (33.3)		

Note: BMI, Body Mass Index; ECOG PS, Eastern Cooperative Oncology Group Performance Status; COPD, Chronic Obstructive Pulmonary Disease; PVTT, Portal Vein Tumor Thrombus; BCLC, Barcelona Clinic Liver Cancer staging; AFP, Alpha-fetoprotein; TB, Total Bilirubin; PLT, Platelet count; MPV, Mean Platelet Volume; PDW, Platelet Distribution Width; mFI-5, modified 5-item frailty index.

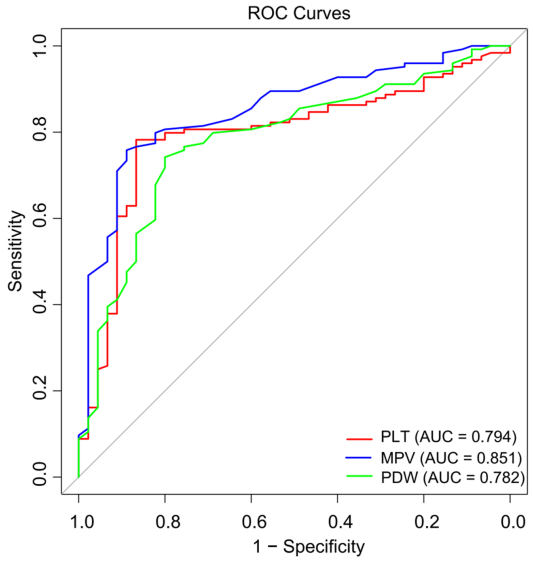

Figure 2. ROC curve for platelet parameters. ROC, Receiver Operating Characteristic; AUC, Area Under Curve; PLT, Platelet count; MPV, Mean Platelet Volume; PDW, Platelet Distribution Width.

associations between the PIS score and clinical characteristics revealed that patients who were aged ≥ 60 years, had Child-Pugh class B, presented with portal vein tumor thrombus, had a maximum tumor diameter ≥ 5 cm, had multiple tumor nodules, or had AFP ≥ 200 μg/L had significantly higher PIS scores ($P < 0.05$) (**Table 3**). Kaplan-Meier curves showed that a higher PIS score was associated with shorter OS and PFS (**Figures 3D**, **4D**). Similarly, a higher mFI-5 score was also associated with shorter OS and PFS (**Figures 3E**, **4E**).

To overcome the subjectivity associated with simple equally weighted summation, we first examined the interaction between mFI-5 and PIS. The results showed no significant interaction between mFI-5 and PIS (**Tables 4**, **5**). Accordingly, we constructed a weighted combined score, designated mFI-5+PIS, by weighting the two indices based on their regression coefficients as follows: mFI-5+PIS: mFI-5+PIS = β_{mFI}×mFI-5+β_{PIS}×PIS.

Analysis of factors influencing OS and PFS

OS: In the training set, the median OS was 10.8 months, with 1 year and 3 year OS rates of

Table 2. Association between platelet parameters and clinical characteristics

Clinical Characteristic	Low PLT Group (n = 102)	High PLT Group (n = 66)	*P* Value	Low MPV Group (n = 70)	High MPV Group (n = 98)	*P* Value	Low PDW Group (n = 68)	High PDW Group (n = 100)	*P* Value
Sex			0.418			0.200			0.516
Female	84 (82.4)	51 (77.3)		53 (75.7)	82 (83.7)		53 (77.9)	82 (82.0)	
Male	18 (17.6)	15 (22.7)		17 (24.3)	16 (16.3)		15 (22.1)	18 (18.0)	
Age (years)			0.066			0.035			0.033
< 60	47 (46.1)	40 (60.6)		43 (61.4)	44 (44.9)		42 (61.8)	26 (38.2)	
≥ 60	55 (53.9)	26 (39.4)		27 (38.6)	54 (55.1)		45 (45.0)	55 (55.0)	
BMI (kg/m^2)			0.942			0.973			0.556
< 25	83 (81.4)	54 (81.8)		57 (81.4)	80 (81.6)		54 (79.4)	83 (83.0)	
≥ 25	19 (18.6)	12 (18.2)		13 (18.6)	18 (18.4)		14 (20.6)	17 (17.0)	
ECOG PS			0.555			0.270			0.202
0	32 (31.4)	19 (28.8)		22 (31.4)	29 (29.6)		22 (32.4)	29 (29.0)	
1	65 (63.7)	41 (62.1)		41 (58.6)	65 (66.3)		39 (57.4)	67 (67.0)	
2	5 (4.9)	6 (9.1)		7 (10.0)	4 (4.1)		7 (10.3)	4 (4.0)	
Child-Pugh			0.001			0.003			0.015
A	81 (79.4)	64 (97.0)		67 (95.7)	78 (79.6)		64 (94.1)	81 (81.0)	
B	21 (20.6)	2 (3.0)		3 (4.3)	20 (20.4)		4 (5.9)	19 (19.0)	
Portal vein tumor thrombus			< 0.001			< 0.001			< 0.001
No	45 (44.1)	51 (77.3)		55 (78.6)	41 (41.8)		52 (76.5)	44 (44.0)	
Yes	57 (55.9)	15 (22.7)		15 (21.4)	57 (58.2)		16 (23.5)	56 (56.0)	
BCLC			0.107			0.373			0.427
A	13 (12.7)	3 (4.5)		6 (8.6)	10 (10.2)		6 (8.8)	10 (10.0)	
B	59 (57.8)	36 (54.5)		36 (51.4)	59 (60.2)		35 (51.5)	60 (60.0)	
C	30 (29.4)	27 (40.9)		28 (40.0)	29 (29.6)		27 (39.7)	30 (30.0)	
Max tumor diameter			< 0.001			0.001			0.008
< 5 cm	65 (63.7)	60 (90.9)		61 (87.1)	64 (65.3)		58 (85.3)	67 (67.0)	
≥ 5 cm	37 (36.3)	6 (9.1)		9 (12.9)	34 (34.7)		10 (14.7)	33 (33.0)	
Number of tumors			0.118			0.013			0.018
Single	27 (26.5)	25 (37.9)		29 (41.4)	23 (23.5)		28 (41.2)	24 (24.0)	
Multiple	75 (73.5)	41 (62.1)		41 (58.6)	75 (76.5)		40 (58.8)	76 (76.0)	
Cirrhosis			0.316			0.781			0.936
No	21 (20.6)	18 (27.3)		17 (24.3)	22 (22.4)		16 (23.5)	23 (23.0)	
Yes	81 (79.4)	48 (72.7)		53 (75.7)	76 (77.6)		52 (76.5)	77 (77.0)	

Ascites			0.538			0.343			0.254
No	77 (75.5)	47 (71.2)		49 (70.0)	75 (76.5)		47 (69.1)	77 (77.0)	
Yes	25 (24.5)	19 (28.8)		21 (30.0)	23 (23.5)		21 (30.9)	23 (23.0)	
Cause of disease			0.207			0.606			0.122
Hepatitis B virus	79 (77.5)	43 (65.2)		48 (68.6)	74 (75.5)		49 (72.1)	73 (73.0)	
Hepatitis C virus	7 (6.9)	8 (12.1)		7 (10.0)	8 (8.2)		3 (4.4)	12 (12.0)	
Others	16 (15.7)	15 (22.7)		15 (21.4)	16 (16.4)		16 (23.5)	15 (15.0)	
AFP (ug/L)			< 0.001			< 0.001			< 0.001
< 200	24 (23.5)	36 (54.5)		39 (55.7)	21 (21.4)		35 (51.5)	25 (25.0)	
≥ 200	78 (76.5)	30 (45.5)		31 (44.3)	77 (78.6)		33 (48.5)	75 (75.0)	
TB (μmol/L)			0.226			1.000			0.870
≤ 17	25 (24.5)	11 (16.7)		15 (21.4)	21 (21.4)		15 (22.1)	21 (21.0)	
> 17	77 (75.5)	55 (83.3)		55 (78.6)	77 (78.6)		53 (77.9)	79 (79.0)	
Albumin (g/L)			0.287			0.976			0.828
> 35	80 (78.4)	47 (71.2)		53 (75.7)	74 (75.5)		52 (76.5)	75 (75.0)	
≤ 35	22 (21.6)	19 (28.8)		17 (24.3)	24 (24.5)		16 (23.5)	25 (25.0)	

Note: PLT, Platelet count; MPV, Mean Platelet Volume; PDW, Platelet Distribution Width; BMI, Body Mass Index; ECOG PS, Eastern Cooperative Oncology Group Performance Status; BCLC, Barcelona Clinic Liver Cancer staging; AFP, Alpha-fetoprotein; TB, Total Bilirubin.

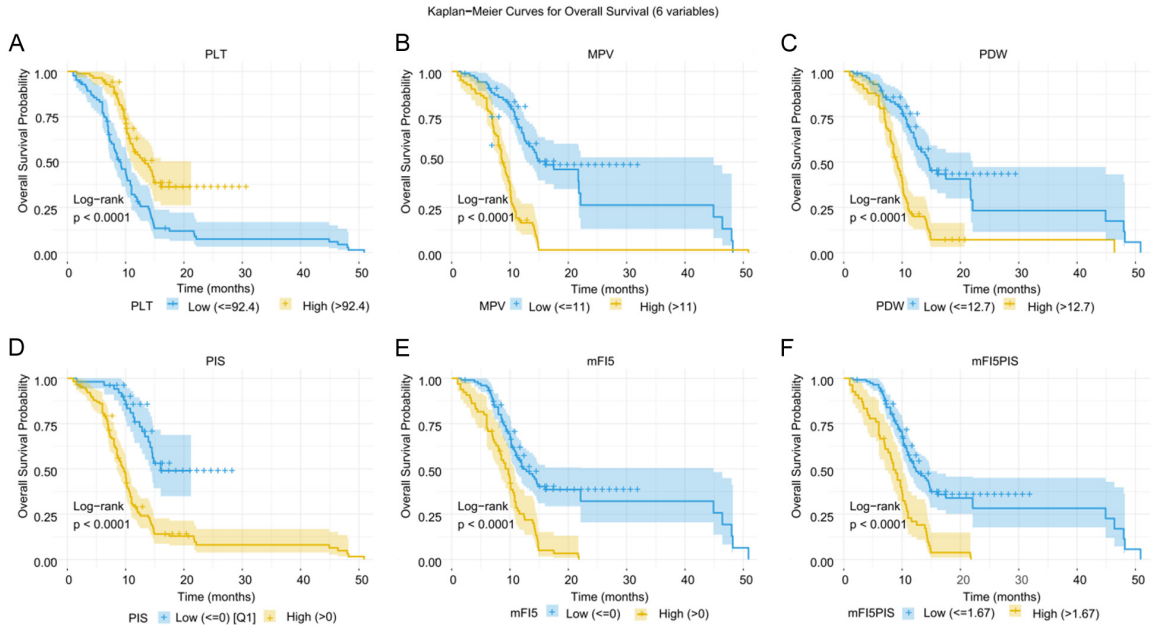

Figure 3. Kaplan-Meier curve of OS. OS, Overall Survival; PLT, Platelet count; MPV, Mean Platelet Volume; PDW, Platelet Distribution Width; PIS, Platelet index score; mFI-5, modified 5-item frailty index.

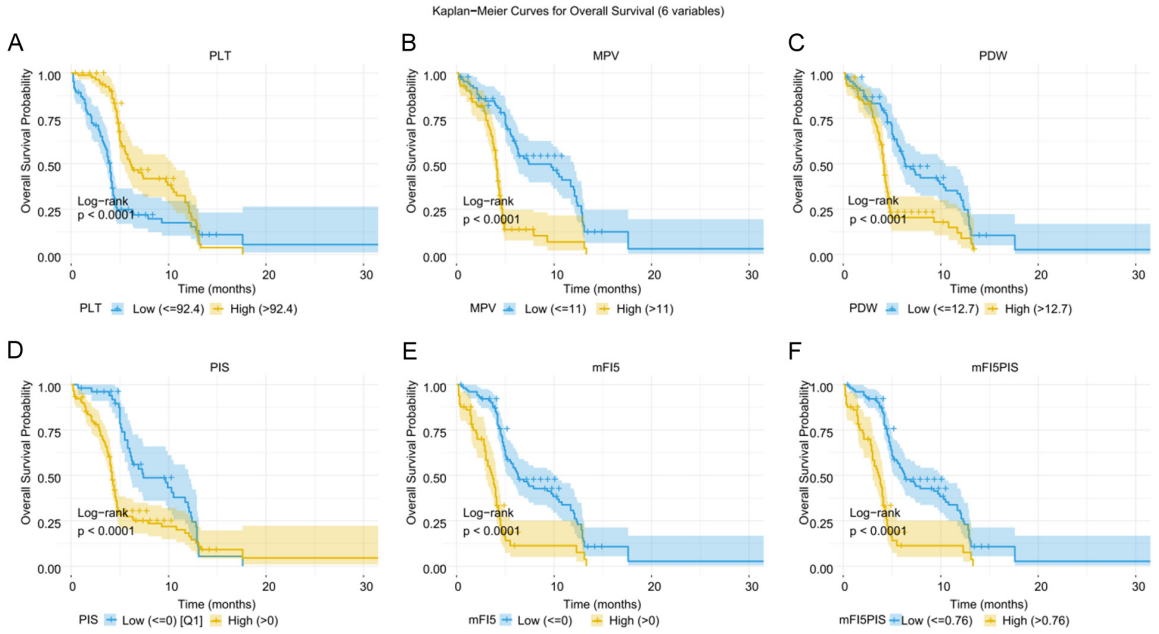

Figure 4. Kaplan-Meier curve of PFS. PFS, Progression-Free Survival; PLT, Platelet count; MPV, Mean Platelet Volume; PDW, Platelet Distribution Width; PIS, Platelet index score; mFI-5, modified 5-item frailty index.

40.9% and 14.5%, respectively. Univariate Cox regression analysis (**Table 6**) showed that age ≥ 60 years, Child-Pugh class B, presence of portal vein tumor thrombus, maximum tumor diameter ≥ 5 cm, multiple tumors, AFP ≥ 200 μg/L, and an increased mFI-5+PIS score were significantly associated with shorter OS (all P < 0.1). These variables were then entered into a multivariate Cox proportional hazards model. The results (**Figure 5A**) confirmed that age ≥ 60 years (HR = 1.6, 95% CI 1.1-2.3, P = 0.022), presence of portal vein tumor thrombus (HR =

Table 3. Association between PIS and clinical characteristics

Clinical Characteristic	PIS 0 (n = 52)	PIS 1 (n = 18)	PIS 2 (n = 11)	PIS 3 (n = 87)	*P* Value
Sex					0.850
Female	40 (76.9)	14 (77.8)	9 (81.8)	72 (82.8)	
Male	12 (23.1)	4 (22.2)	2 (18.2)	15 (17.2)	
Age (years)					0.035
< 60	31 (59.6)	12 (66.7)	8 (72.7)	36 (41.4)	
≥ 60	21 (40.4)	6 (3.3)	3 (27.3)	51 (58.6)	
BMI (kg/m^2)					0.884
< 25	42 (80.8)	14 (77.8)	10 (90.9)	71 (81.6)	
≥ 25	10 (19.2)	4 (22.2)	1 (9.1)	16 (18.4)	
ECOG PS					0.390
0	14 (26.9)	8 (44.4)	5 (45.5)	24 (27.6)	
1	32 (61.5)	9 (50.0)	6 (54.5)	59 (67.8)	
2	6 (11.5)	1 (5.6)	0 (0.0)	4 (4.6)	
Child-Pugh					0.010
A	51 (98.1)	16 (88.9)	10 (90.9)	68 (78.2)	
B	1 (1.9)	2 (11.1)	1 (9.1)	19 (21.8)	
Portal vein tumor thrombus					< 0.001
No	41 (78.8)	14 (77.8)	7 (63.6)	34 (39.1)	
Yes	11 (21.2)	4 (22.2)	4 (36.4)	53 (60.9)	
BCLC					0.279
A	2 (3.8)	4 (22.2)	1 (9.1)	9 (10.3)	
B	28 (53.8)	8 (44.4)	7 (63.6)	52 (59.8)	
C	22 (42.3)	6 (33.3)	3 (27.3)	26 (29.9)	
Max tumor diameter					0.003
< 5 cm	47 (90.4)	14 (77.8)	9 (81.8)	55 (63.2)	
≥ 5 cm	5 (9.6)	4 (22.2)	2 (18.2)	32 (36.8)	
Number of tumors					0.008
Single	19 (36.5)	11 (61.1)	3 (27.3)	19 (21.8)	
Multiple	33 (63.5)	7 (38.9)	8 (72.7)	68 (78.2)	
Cirrhosis					0.654
No	12 (23.1)	6 (33.3)	3 (27.3)	18 (20.7)	
Yes	40 (76.9)	12 (66.7)	8 (72.7)	69 (79.3)	
Ascites					0.285
No	38 (73.1)	10 (55.6)	9 (81.8)	67 (77.0)	
Yes	14 (26.9)	8 (44.4)	2 (18.2)	20 (23.0)	
Cause of disease					0.165
Hepatitis B virus	37 (71.2)	11 (61.1)	6 (54.5)	68 (78.2)	
Hepatitis C virus	3 (5.8)	3 (16.7)	3 (27.3)	6 (6.9)	
Others	12 (23.1)	4 (22.2)	2 (18.2)	13 (14.9)	
AFP (ug/L)					< 0.001
< 200	29 (55.8)	9 (50.0)	5 (45.5)	17 (19.5)	
≥ 200	23 (44.2)	9 (50.0)	6 (54.5)	70 (80.5)	
TB (μmol/L)					0.927
≤ 17	10 (19.2)	4 (22.2)	3 (27.3)	19 (21.8)	
> 17	42 (80.8)	14 (77.8)	8 (72.7)	68 (78.2)	
Albumin (g/L)					0.533
> 35	37 (71.2)	15 (83.3)	10 (90.9)	65 (74.7)	
≤ 35	15 (28.8)	3 (16.7)	1 (9.1)	22 (25.3)	

Note: PIS, Platelet index score; BMI, Body Mass Index; ECOG PS, Eastern Cooperative Oncology Group Performance Status; BCLC, Barcelona Clinic Liver Cancer staging; AFP, Alpha-fetoprotein; TB, Total Bilirubin.

Table 4. Interaction analysis between the mFI-5 and PIS for the OS endpoint

PIS	mFI-5	HR	95% CI
Normal	Non-frail	1.00	1.00
Abnormal	Non-frail	3.15	1.74-5.72
Normal	Frail	2.85	0.82-9.94
Abnormal	Frail	5.43	0.23-129.47
RERI	-	0.43	-3.21-4.00
AP	-	0.08	-0.65-0.60
S	-	1.11	0.53-3.26

Note: OS, Overall Survival; mFI-5, modified 5-item frailty index; PIS, Platelet index score; HR, Hazard Ratio; CI, Confidence Interval; RERI, Relative Excess Risk due to Interaction; AP, Attributable Proportion due to interaction; S, Synergy Index.

Table 5. Interaction analysis between the mFI-5 and PIS for PFS endpoint

PIS	mFI-5	HR	95% CI
Normal	Non-frail	1.00	1.00
Abnormal	Non-frail	1.16	0.73-1.86
Normal	Frail	1.88	0.56-6.30
Abnormal	Frail	3.26	2.04-5.20
RERI	-	1.21	-0.52-5.37
AP	-	0.37	-0.15-0.93
S	-	2.16	-5.06-16.42

Note: PFS, Progression-Free Survival; mFI-5, modified 5-item frailty index; PIS, Platelet index score; HR, Hazard Ratio; CI, Confidence Interval; RERI, Relative Excess Risk due to Interaction; AP, Attributable Proportion due to interaction; S, Synergy Index.

2.0, 95% CI 1.3-3.2, P = 0.001), AFP ≥ 200 μg/L (HR = 2.2, 95% CI 1.4-3.6, P < 0.001), and an increased mFI-5+PIS score (HR = 1.8, 95% CI 1.4-2.4, P < 0.001) were independent adverse predictors of OS. Kaplan-Meier survival curve analysis demonstrated that a higher mFI-5+PIS score (cut off ≤ 1.67) was associated with shorter OS. The survival curve of the high score group was consistently below that of the low score group, and the survival gap between the two groups widened over time. Patients in the high score group showed a rapid decline in survival rate and significantly worse long term survival benefits (Log-rank P < 0.001) (**Figure 3F**).

PFS: In the training set, the median PFS was 4.7 months, and the 1 year PFS rate was 22.0%. Univariate Cox regression analysis (**Table 6**) revealed that age ≥ 60 years, Child-Pugh class B, presence of portal vein tumor thrombus, maximum tumor diameter ≥ 5 cm, multiple tumors, AFP ≥ 200 μg/L, and an increased mFI-5+PIS score were significantly associated with shorter PFS (all P < 0.1). Multivariate Cox regression analysis (**Figure 5B**) showed that presence of portal vein tumor thrombus (HR = 2.8, 95% CI 1.9-4.2, P < 0.001), AFP ≥ 200 μg/L (HR = 2.1, 95% CI 1.4-3.3, P < 0.001), maximum tumor diameter ≥ 5 cm (HR = 1.6, 95% CI 1.0-2.4, P = 0.031), Child-Pugh class B (HR = 2.4, 95% CI 1.4-4.0, P < 0.001), multiple tumors (HR = 1.6, 95% CI 1.1-2.5, P = 0.025), and an increased mFI-5+PIS score (HR = 2.2, 95% CI 1.6-3.1, P < 0.001) were independent predictors of PFS. Kaplan-Meier survival curve analysis indicated that a higher mFI-5+PIS score was associated with shorter PFS (Log-rank P < 0.001), with good curve separation (**Figure 4F**).

Nomogram construction and validation

Based on the multivariate analysis results for OS and PFS, nomograms were constructed (**Figure 6A**, **6B**). In the training cohort, the C index for OS of the multivariate prognostic model based only on portal vein tumor thrombus, AFP, and age was 0.771, which increased to 0.795 after incorporating mFI-5+PIS. For PFS, the C index of the multivariate prognostic model based only on portal vein tumor thrombus, AFP, maximum tumor diameter, Child-Pugh class, and number of tumors was 0.794, which increased to 0.821 after including mFI-5+PIS. Calibration curves (**Figure 7A**, **7B**) showed that the 1 year and 3 year OS rates and the 1 year PFS rate predicted by the nomograms were in good agreement with the actual observed values, without significant deviation, indicating excellent model calibration. Time-dependent ROC curves (**Figure 7C**, **7D**) demonstrated that the combined model incorporating the mFI-5+PIS score had a significantly higher AUC for predicting OS than the model without the combined score. Similarly, the AUC for predicting 1 year PFS was also higher than that of the model without the combined score.

In the internal validation cohort, the C indices for PFS were 0.770 and 0.801 without and with mFI-5+PIS, respectively. The C indices for OS were 0.754 and 0.822 without and with mFI-

Table 6. Univariate Cox regression analysis

Variable	OS		PFS	
	HR (95% CI)	*P* value	HR (95% CI)	*P* value
Sex				
Female	1 (Reference)		1 (Reference)	
Male	0.78 (0.49-1.25)	0.304	0.82(0.53-1.28)	0.387
Age (years)				
< 60	1 (Reference)		1 (Reference)	
≥ 60	2.18 (1.50-3.16)	< 0.001	2.01(1.41-2.84)	< 0.001
BMI (kg/m^2)				
< 25	1 (Reference)		1 (Reference)	
≥ 25	1.11 (0.69-1.78)	0.678	1.06(0.7-1.62)	0.775
ECOG PS				
0	1 (Reference)		1 (Reference)	
1	1.08 (0.72-1.61)	0.704	1.04(0.72-1.51)	0.843
2	0.98 (0.47-2.05)	0.966	0.72(0.34-1.53)	0.394
Child-Pugh				
A	1 (Reference)		1 (Reference)	
B	2.83 (1.75-4.57)	< 0.001	4.06 (2.47-6.68)	0
Portal vein tumor thrombus				
No	1 (Reference)		1 (Reference)	
Yes	4.74 (3.22-6.98)	< 0.001	5.15 (3.54-7.49)	< 0.001
BCLC				
A	1 (Reference)		1 (Reference)	
B	1.04 (0.54-2.03)	0.899	0.79 (0.43-1.47)	0.463
C	1.02 (0.51-2.05)	0.961	0.76 (0.4-1.44)	0.398
Max tumor diameter				
< 5 cm	1 (Reference)		1 (Reference)	
≥ 5 cm	1.94 (1.31-2.87)	0.001	2.52 (1.7-3.73)	< 0.001
Number of tumors				
Single	1 (Reference)			
Multiple	1.41 (0.95-2.09)	0.089	1.99 (1.34-2.94)	0.001
Cirrhosis				
No	1 (Reference)		1 (Reference)	
Yes	0.95 (0.62-1.46)	0.829	1.11 (0.74-1.66)	0.618
Ascites				
No	1 (Reference)			
Yes	0.78 (0.51-1.18)	0.233	0.89 (0.6-1.3)	0.544
Cause of disease				
Hepatitis B virus	1 (Reference)		1 (Reference)	
Hepatitis C virus	0.67 (0.35-1.28)	0.225	0.77 (0.42-1.41)	0.403
Others	0.97 (0.59-1.60)	0.918	0.89 (0.56-1.4)	0.617
AFP (ug/L)				
< 200	1 (Reference)		1 (Reference)	
≥ 200	3.99 (2.60-6.13)	< 0.001	2.52 (1.7-3.73)	< 0.001
TB (μmol/L)				
≤ 17	1 (Reference)		1 (Reference)	
> 17	0.86 (0.57-1.31)	0.492	1.18 (0.76-1.84)	0.457
Albumin (g/L)				
> 35	1 (Reference)		1 (Reference)	
≤ 35	1.24 (0.82-1.86)	0.303	1.28 (0.85-1.91)	0.237
mFI-5+PIS	2.68 (2.05-3.50)	< 0.001	3.01 (2.21-4.09)	< 0.001

Note: OS, Overall Survival; PFS, Progression-Free Survival; HR, Hazard Ratio; CI, Confidence Interval; BMI, Body Mass Index; ECOG PS, Eastern Cooperative Oncology Group Performance Status; BCLC, Barcelona Clinic Liver Cancer staging; AFP, Alpha-fetoprotein; TB, Total Bilirubin; mFI-5+PIS, combined modified 5-item frailty index and platelet index score.

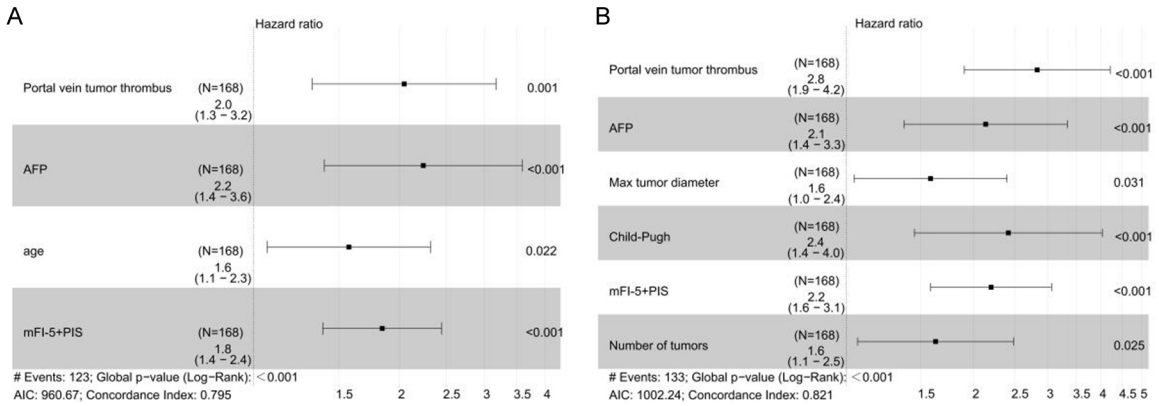

Figure 5. Multifactorial analysis risk forest plot. A. OS. B. PFS. OS, Overall Survival; PFS, Progression-Free Survival; HR, Hazard Ratio; CI, Confidence Interval; AFP, Alpha-fetoprotein; AIC, Akaike Information Criterion; C-index, Concordance index; mFI-5+PIS, combined modified 5-item frailty index and platelet index score.

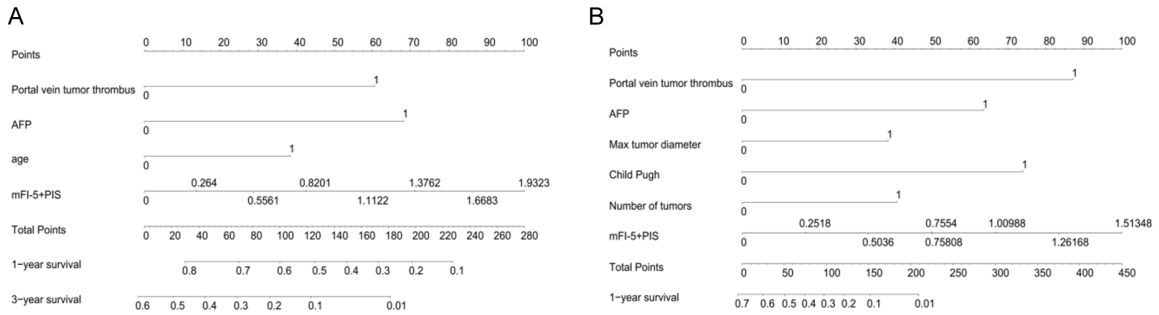

Figure 6. Nomogram. A. OS. B. PFS. OS, Overall Survival; PFS, Progression-Free Survival; AFP, Alpha-fetoprotein; mFI-5+PIS, combined modified 5-item frailty index and platelet index score.

5+PIS, respectively. Calibration curves (**Figure 8A**, **8B**) showed that the 1 year and 3 year OS rates and the 1 year PFS rate predicted by the nomograms in the validation cohort fitted well with the actual observed values, with no obvious deviation from the ideal diagonal. Time-dependent ROC curve analysis (**Figure 8C**, **8D**) revealed that in the validation cohort, the combined model incorporating the mFI-5+PIS score had significantly higher AUC values for predicting 1 year and 3 year OS and 1 year PFS than the base model without the combined score.

In the external validation cohort, the C-index for PFS without and with the mFI-5+PIS score was 0.731 and 0.771, respectively; for OS, the corresponding values were 0.620 and 0.748. Calibration curves of the nomogram (**Figure 9A** and **9B**) demonstrated good agreement between the predicted 1-year and 3-year OS rates and 1-year PFS rates and the actual observed values, indicating satisfactory calibration. Time-dependent ROC curve analysis (**Figure 9C** and **9D**) showed that the combined model incorporating the mFI-5+PIS score achieved higher AUC values for predicting 1-year and 3-year OS and 1-year PFS compared with the baseline model without the combined score.

Subgroup analysis

To comprehensively evaluate the predictive robustness of the mFI-5+PIS score across different clinical settings, we performed subgroup analyses stratified by etiology, treatment regimen, portal vein tumor thrombus (PVTT) status, and maximum tumor diameter, and further conducted interaction tests. The results demonstrated that the mFI-5+PIS score effectively stratified patients into high- and low-risk groups for both overall survival (OS) and progression-free survival (PFS) among patients with HBV, HCV, and other etiologies, among those receiv-

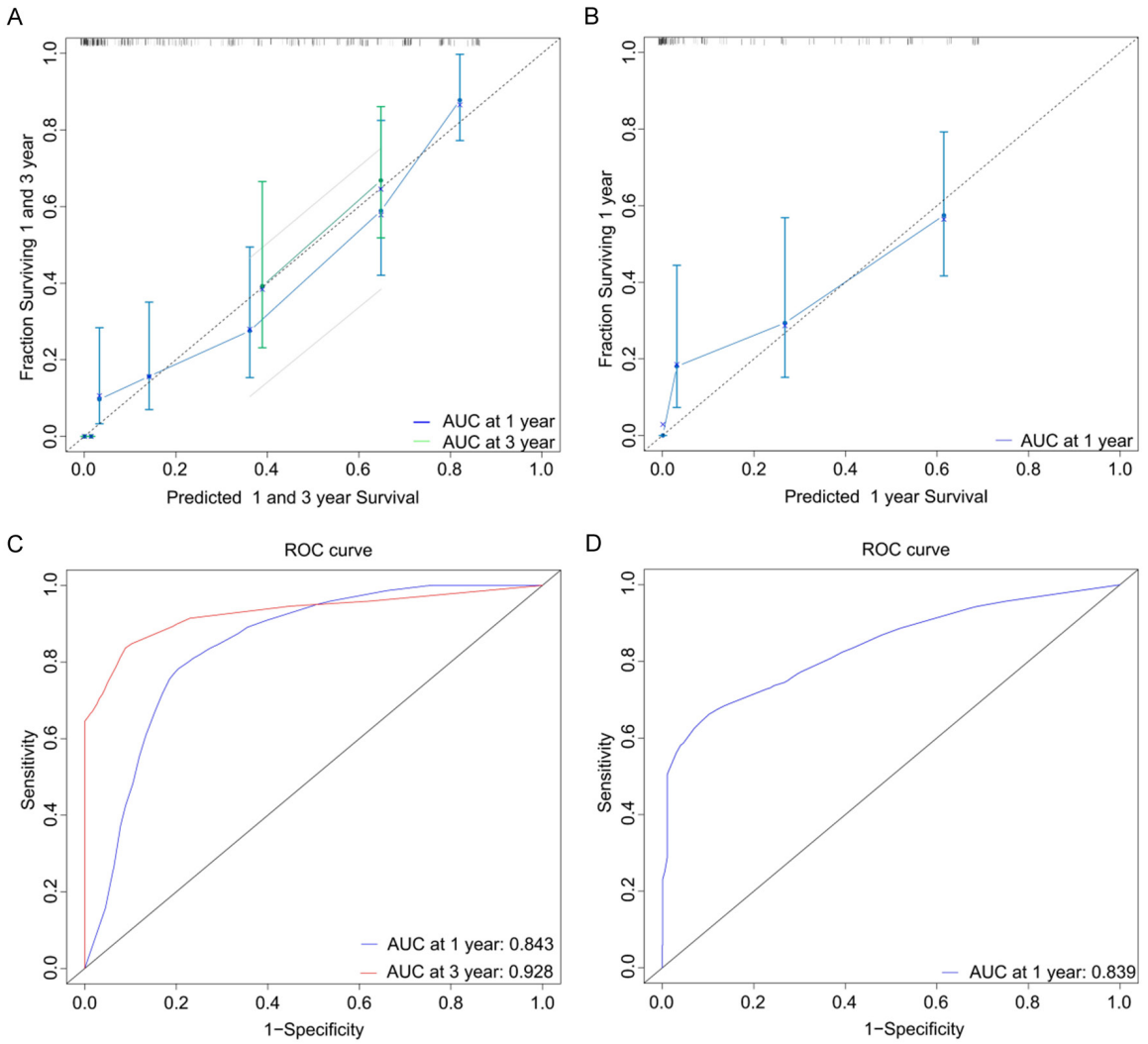

Figure 7. Calibration curves and ROC curves of the models in the training cohort. A. Calibration curve of the OS model. B. Calibration curve of the PFS model. C. ROC curve of the OS model. D. ROC curve of the PFS model. OS, Overall Survival; PFS, Progression-Free Survival.

ing TACE alone or TACE combined with targeted therapy and immunotherapy, and among those with or without PVTT, as well as those with maximum tumor diameter ≥ 5 cm or < 5 cm (all subgroup Log-rank P < 0.05) (**Figures 10** and **11**). We further examined the interaction between the mFI-5+PIS score (as a continuous variable) and key clinical factors using Cox proportional hazards models with product interaction terms in the overall cohort. The results showed that for the OS endpoint, neither PVTT status (P_interaction = 0.061) nor tumor size (P_interaction = 0.166) significantly modified the prognostic effect of the mFI-5+PIS score; for the PFS endpoint, the interaction *P* values for PVTT (P_interaction = 0.143) and tumor size (P_interaction = 0.305) were also > 0.05. Within each subgroup, the hazard ratios (HRs) of the mFI-5+PIS score for both OS and PFS were consistently > 1 with P < 0.01, further confirming the significant prognostic value of the score across all subgroups.

Discussion

In recent years, the epidemiological burden of HCC has continued to increase [2]. TACE remains a key locoregional therapy for patients who are not candidates for resection or ablation; however, even with the same treatment, patient outcomes vary widely [16, 17]. In clinical practice, more accurate risk stratification

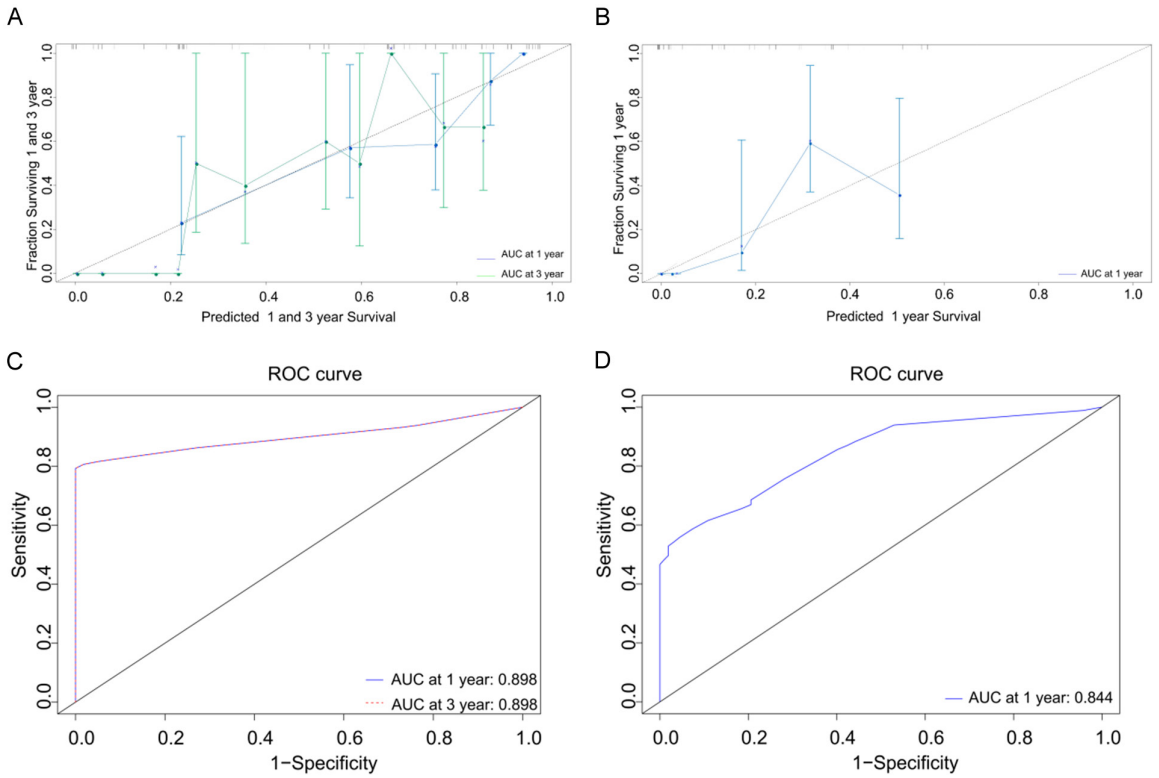

Figure 8. Calibration curves and ROC curves of the models in the internal validation cohort. A. Calibration curve of the OS model. B. Calibration curve of the PFS model. C. ROC curve of the OS model. D. ROC curve of the PFS model. ROC, Receiver Operating Characteristic; AUC, Area Under Curve; OS, Overall Survival; PFS, Progression-Free Survival.

tools are urgently needed to guide the formulation of treatment plans and the implementation of follow-up strategies. Previous studies have shown that the state of frailty can independently predict the overall survival of elderly tumor patients [18]. At the same time, platelet-related indicators such as PLT are closely related to tumor invasion and prognosis. An increase in platelet levels often suggests that the survival outcome of patients is worse [19, 20]. However, there is no study to combine the state of frailty with platelet indicators to predict the long-term prognosis of patients with HCC treated with TACE. This study constructs a new composite scoring model, combining the mFI-5 with the PIS integrating PLT, MPV and PDW. The research results confirm that the mFI-5+PIS composite score can independently predict OS and PFS of patients. In addition, the composite score significantly improves the discriminative efficiency of the nomogram model, helping to more accurately identify high-risk patients - such patients have a higher risk of death or disease progression after receiving TACE treatment.

The mFI-5 can reflect the patient's overall physiological reserve level and multisystemic comorbidity burden, and the comorbidity status itself has been proven to increase the risk of perioperative complications and long-term death [21-23]. A study on patients with HCC found that frail patients treated with TACE (mFI-5 score ≥ 2) had a significantly shorter OS and PFS than those of non-frail patients, suggesting that frailty and poor recovery of liver function are closely related to a poor prognosis [10]. For patients with HCC, repeated TACE treatment may reduce the treatment effect and induce liver function damage, and the deterioration of liver function is a key factor limiting the continuity of treatment [24]. The state of frailty may reduce the liver's tolerance to TACE-related ischemia-reperfusion injury, resulting in a slow recovery of liver function after each treatment, thus limiting the cumulative number of treatments, and ultimately affecting the long-term control effect of the tumor. In addition, the state of frailty also weakens the patient's tolerance to adverse reactions to subsequent systemic treatment (such as targeted

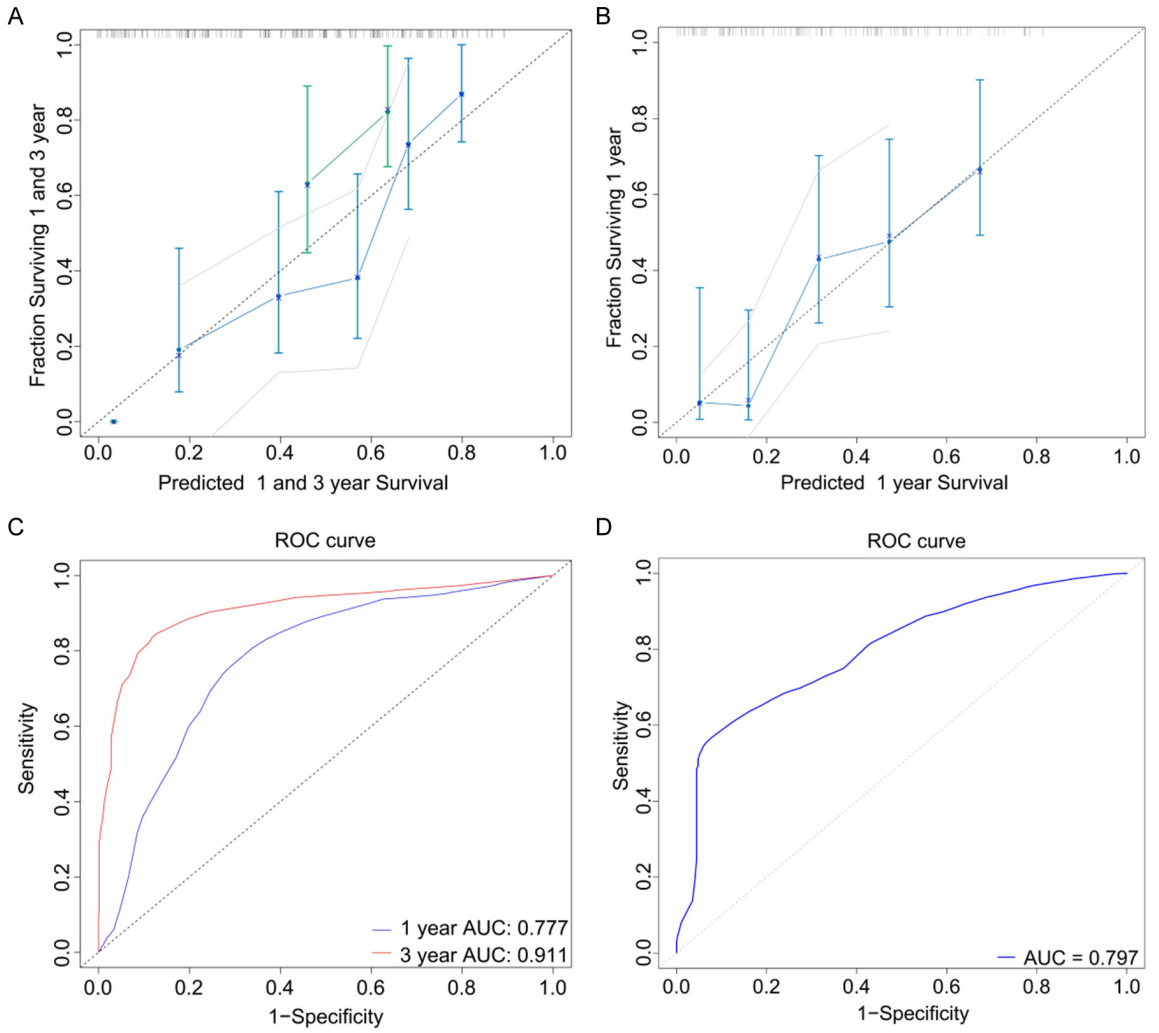

Figure 9. Calibration curves and ROC curves of the models in the external validation cohort. A. Calibration curve of the OS model. B. Calibration curve of the PFS model. C. ROC curve of the OS model. D. ROC curve of the PFS model. ROC, Receiver Operating Characteristic; AUC, Area Under Curve; OS, Overall Survival; PFS, Progression-Free Survival.

therapy or immunotherapy), making it difficult to fully implement combined treatment or sequential treatment strategies [25]. Therefore, frail patients are more prone to liver decompensation, infection or cardiopulmonary complications when receiving invasive treatments such as TACE - such treatments are often accompanied by systemic stress responses, such as post-embolization syndrome [10, 26]. Even if the tumor control effect is similar, OS of such patients may still be shortened by aggravation of underlying diseases or non-tumor-related deaths. The conclusion of this study is consistent with this trend, further confirming that the frailty index can be used to predict the survival outcome of patients with HCC after treatment.

PIS is composed of three indicators: PLT, MPV and PDW, which can reflect the quantitative characteristics and activation status of platelets at the same time. The prognostic value of this score mainly comes from the complex role played by platelets in the development of tumors. Activated platelets will release transforming growth factor-β (TGF-β), which can induce epithelial-mesenchymal transition (EMT) of tumor cells, promoting tumor cell infiltration and distant metastasis; at the same time, platelet-derived growth factor can support the formation of tumor microenvironment and the proliferation of tumor cells [27, 28]. The increase in MPV and PDW is a manifestation of enhanced platelet activation, suggesting that the body is in a state of systemic high inflam-

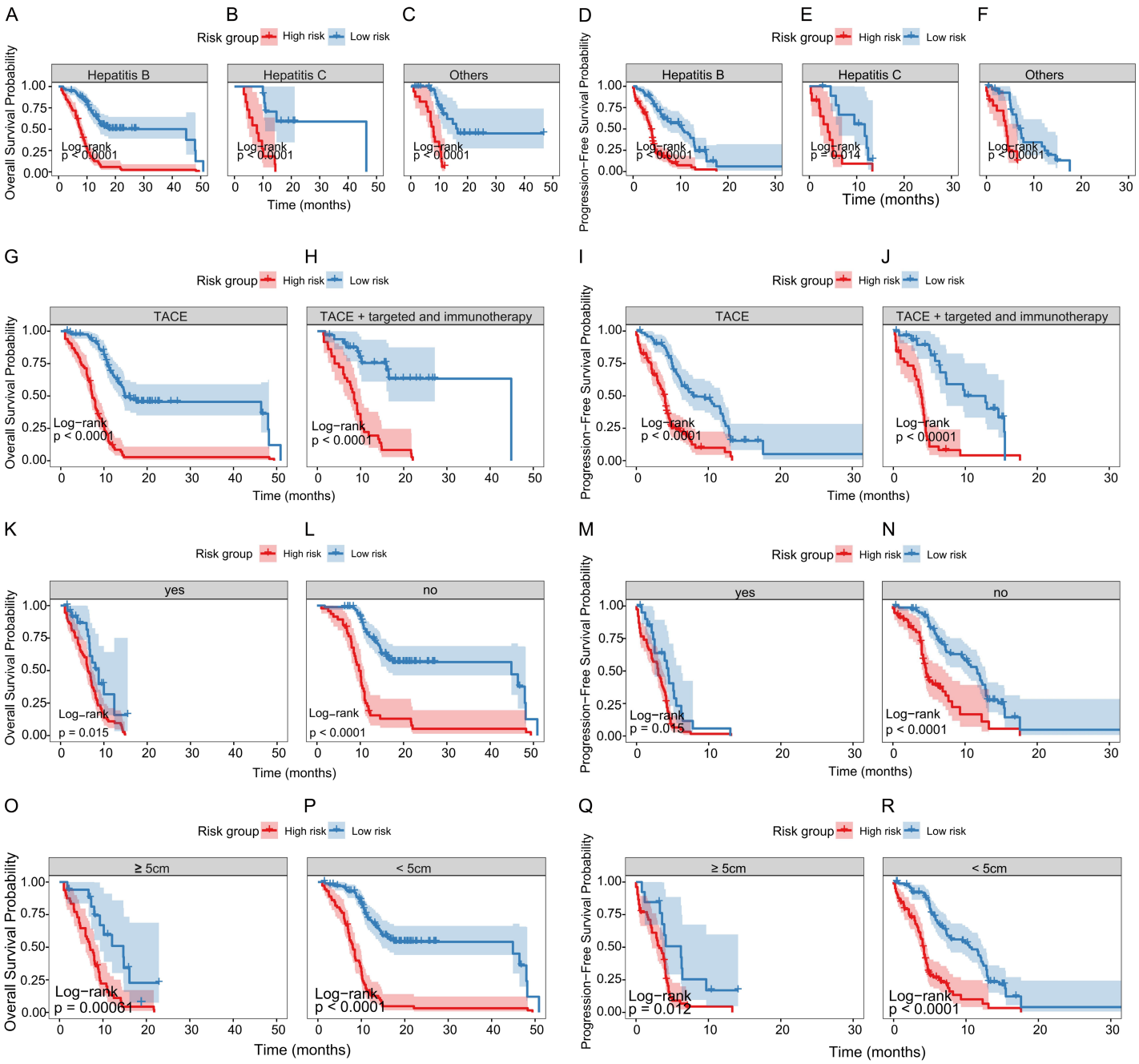
A
B
C
D
E
F
Risk group
High risk
Low risk
Hepatitis B
Hepatitis C
Others
Overall Survival Probability
Progression−Free Survival Probability
Log−rank p < 0.0001
Log−rank p < 0.0001
Log−rank p < 0.0001
Log−rank p < 0.0001
Log−rank p = 0.014
Log−rank p < 0.0001
Time (months)
G
H
I
J
TACE
TACE + targeted and immunotherapy
Log−rank p < 0.0001
Log−rank p < 0.0001
Log−rank p < 0.0001
Log−rank p < 0.0001
K
L
M
N
yes
no
Log−rank p = 0.015
Log−rank p < 0.0001
Log−rank p = 0.015
Log−rank p < 0.0001
O
P
Q
R
≥ 5cm
< 5cm
Log−rank p = 0.00061
Log−rank p < 0.0001
Log−rank p = 0.012
Log−rank p < 0.0001

Figure 10. Subgroup analyses of the OS and PFS models in the overall cohort. A-C. Kaplan-Meier survival curves for the OS model stratified by etiology. D-F. Kaplan-Meier survival curves for the PFS model stratified by etiology. G, H. Kaplan-Meier survival curves for the OS model stratified by treatment regimen. I, J. Kaplan-Meier survival curves for the PFS model stratified by treatment regimen. K, L. Kaplan-Meier survival curves for the OS model stratified by portal vein tumor thrombus status. M, N. Kaplan-Meier survival curves for the PFS model stratified by portal vein tumor thrombus status. O, P. Kaplan-Meier survival curves for the OS model stratified by maximum tumor diameter. Q, R. Kaplan-Meier survival curves for the PFS model stratified by maximum tumor diameter.

mation and hypercoagulation [29, 30]. After treatment with TACE, residual tumor cells will release angiogenesis signals; if the patient himself already has a state of platelet hyperactivation (manifested by MPV and PDW), it may further accelerate the process of tumor vascular reconstruction and recurrence [31-33]. In addition, platelets can also encircle circulating tumor cells, helping them escape the attack of the immune system, thereby promoting metastasis. Not only that, platelets can inhibit the activity of natural killer cells (NK cells) and T cells by releasing immunosuppressive factors, thereby interacting with the immune system to form an immunosuppressive microenvironment. This microenvironment may weaken the anti-tumor immune response after TACE treatment and affect the efficacy of subsequent immunotherapy [34, 35]. As a comprehensive scoring system, PIS can simultaneously reflect the interaction between tumor load, liver function and systemic inflammation-coagulation state, providing a new risk stratification method based on routine blood testing for patients with HCC treated with TACE.

Building on this, we weighted mFI-5 and PIS using multivariate Cox regression coefficients to establish a novel combined score, designated mFI-5+PIS, which simultaneously reflects the patient's overall physiological reserve, comorbidity burden, and systemic inflammatory and coagulation activation status. The results showed that mFI-5+PIS had strong independent predictive ability for both OS and PFS, with hazard ratios increasing significantly as the score increased. The predictive value of mFI-5+PIS likely stems from the potential synergistic mechanisms between frailty and platelet activation in the progression of hepatocellular carcinoma and treatment response. Frailty, as assessed by mFI-5, is essentially a comprehensive manifestation of multisystem physiological decline and increased vulnerability, reflecting a reduced physiological reserve and heightened susceptibility to stressors. Frail patients often present with low-grade chronic systemic inflammation, characterized by elevated levels of inflammatory factors such as interleukin-6 (IL-6), tumor necrosis factor-α (TNF-α), and C-reactive protein (CRP) [36, 37]. These inflammatory cytokines can stimulate the liver to produce thrombopoietin (TPO), promoting megakaryocyte proliferation and platelet production, while also activating platelets, leading to increased MPV and PDW [38]. Activated platelets, in turn, release inflammatory mediators that amplify the inflammatory response [39, 40]. Consequently, frail patients are more sensitive to the poor prognosis reflected by the PIS. However, previous studies have mostly evaluated frailty or platelet indicators separately, and even when frailty was combined with other indicators, it was often through simple summation [41]. In contrast, our study integrated frailty status with platelet activation status through a weighted combined score, achieving more refined risk stratification for patients with HCC undergoing TACE. Zhu et al. [42] constructed a nomogram model based on the PIS and found that low PLT, high MPV, and high PDW were significantly associated with postoperative recurrence of HCC; however, that study only included platelet indicators without considering the patient's overall physiological reserve. Chronic low grade inflammation is not only a driver of tumor progression but is also closely associated with frailty. Cibeira et al. [43] demonstrated through a cross sectional study in a Spanish elderly population that inflammatory biomarkers such as CRP, TNF-α, sTNF-RII, and GDF15 were significantly positively correlated with physical frailty, with sTNF-RII showing particularly outstanding predictive ability, while CRP and TNF-α could effectively distinguish prefrail individuals. A large scale prospective cohort study by Zhang et al. [18] confirmed that elevated systemic inflammation levels were significantly positively associated with frailty (OR = 1.23, 95% CI 1.08-1.41), and patients with both frailty and elevated inflammation had the highest overall mortality risk (HR = 1.83, 95% CI 1.59-2.04), significantly higher than those with only a single risk factor.

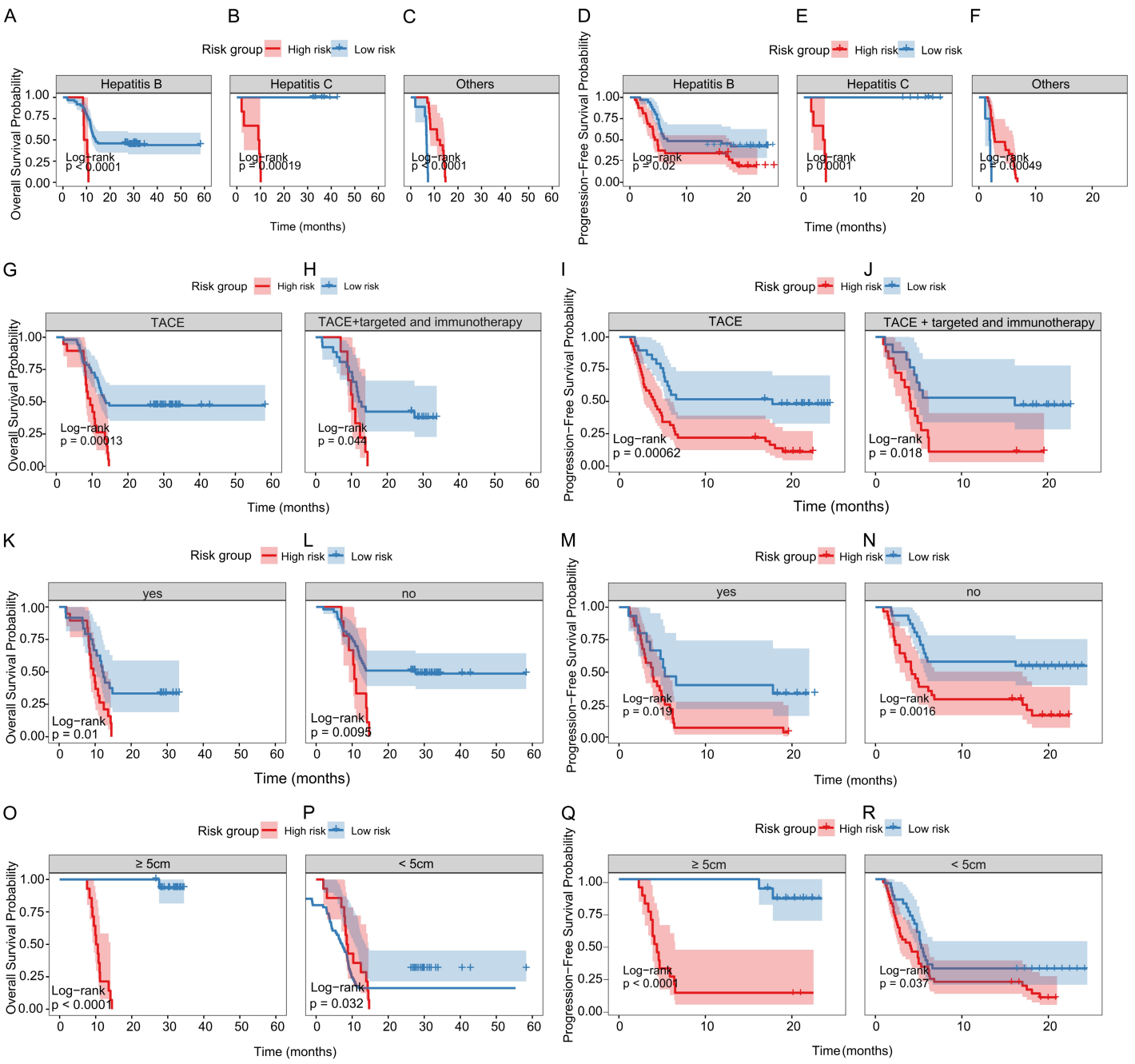
A
B
C
D
E
F
Risk group High risk Low risk
Hepatitis B
Hepatitis C
Others
Overall Survival Probability
Progression−Free Survival Probability
Log−rank p < 0.0001
Log−rank p = 0.00019
Log−rank p < 0.0001
Log−rank p = 0.02
Log−rank p = 0.0001
Log−rank p = 0.00049
Time (months)
G
H
I
J
TACE
TACE+targeted and immunotherapy
TACE + targeted and immunotherapy
Log−rank p = 0.00013
Log−rank p = 0.044
Log−rank p = 0.00062
Log−rank p = 0.018
K
L
M
N
yes
no
Log−rank p = 0.01
Log−rank p = 0.0095
Log−rank p = 0.019
Log−rank p = 0.0016
O
P
Q
R
≥ 5cm
< 5cm
Log−rank p < 0.0001
Log−rank p = 0.032
Log−rank p < 0.0001
Log−rank p = 0.037

Figure 11. Subgroup analyses of the OS and PFS models in the external validation cohort. A-C. Kaplan-Meier survival curves for the OS model stratified by etiology in the external validation cohort. D-F. Kaplan-Meier survival curves for the PFS model stratified by etiology in the external validation cohort. G, H. Kaplan-Meier survival curves for the OS model stratified by treatment regimen in the external validation cohort. I, J. Kaplan-Meier survival curves for the PFS model stratified by treatment regimen in the external validation cohort. K, L. Kaplan-Meier survival curves for the OS model stratified by portal vein tumor thrombus status in the external validation cohort. M, N. Kaplan-Meier survival curves for the PFS model stratified by portal vein tumor thrombus status in the external validation cohort. O, P. Kaplan-Meier survival curves for the OS model stratified by maximum tumor diameter in the external validation cohort. Q, R. Kaplan-Meier survival curves for the PFS model stratified by maximum tumor diameter in the external validation cohort.

In our study, patients in the high risk group of the combined score often presented with both underlying frailty and abnormal platelet activation indicators, which is consistent with the findings of Zhang et al. [18]. In the present cohort, a higher PIS score was significantly associated with adverse features including age ≥ 60 years, Child-Pugh class B, presence of portal vein tumor thrombus, maximum tumor diameter ≥ 5 cm, multiple tumors, and AFP ≥ 200 μg/L ($P < 0.05$); these features are either components of, or important contributors to, frailty. Therefore, mFI-5+PIS can assess patient risk from the dimensions of physical vulnerability and systemic inflammation, hypercoagulability, and tumor burden.

In this study, subgroup analyses and interaction tests were performed to further validate the clinical robustness of the score. The results demonstrated that the mFI-5+PIS score consistently identified high-risk patients across subgroups stratified by etiology, treatment regimen, portal vein tumor thrombus (PVTT) status, and tumor size, and its prognostic effect was not modified by PVTT or tumor size (all P_interaction > 0.05). This finding carries important clinical implications. In clinical decision-making for HCC, PVTT and tumor size are recognized as key prognostic factors [44-46]; however, the mFI-5+PIS score provides additional and independent risk information beyond these factors, suggesting that it may serve as an effective complementary tool to existing staging systems. This is particularly valuable for patient populations with substantial heterogeneity within the same clinical subgroup, facilitating more refined individualized prognostic assessment. Moreover, the consistency of the prognostic effect across subgroups rules out potential confounding effects on model accuracy, further reinforcing the reliability of our findings.

In recent years, research on the association between frailty and tumor prognosis has increasingly delved into molecular mechanisms. Frailty itself is a multifactorial syndrome, with underlying molecular mechanisms including chronic low-grade inflammation, dysregulation of muscle protein metabolism, mitochondrial dysfunction, and hormonal and metabolic disturbances. These mechanisms remarkably overlap with the pathogenic pathways of hepatocellular carcinoma (HCC), particularly in the context of cirrhosis or metabolic dysfunction-associated steatohepatitis (MASH) [47]. In this context, cellular senescence serves as both a core molecular basis of frailty and a critical driver of HCC development and progression. On the one hand, senescent cells release abundant inflammatory cytokines through the senescence-associated secretory phenotype (SASP), reshaping the hepatic microenvironment, promoting fibrosis, and suppressing immune responses, thereby creating a permissive condition for HCC initiation [48]. On the other hand, under oncogenic stress, some senescent hepatocytes can "escape" the senescent state through metabolic reprogramming (e.g., downregulation of FBP1, activation of the NRF2/AKT pathway, and accelerated p53 degradation) and acquire progenitor-like characteristics, directly participating in tumor initiation [48]. Frailty-related systemic and persistent low-grade inflammation is not only a core driver of physical functional decline but also a major contributor to malignancy progression, and HCC is a prototypical inflammation-associated cancer [37, 49, 50]. Primary HCC typically arises in fibrotic livers, where persistent inflammation and extracellular matrix remodeling create a favorable environment for the malignant transformation of normal cells [51]. Platelets also play an important role in this chronic inflammation-driven process of hepatocarcinogenesis. Activated platelets can promote tumor cell proliferation and facilitate tumor-stromal interactions that drive tumor progression [52]. Platelets can also directly interact with HCC cells by activating the TLR4/NF-κB signaling

pathway on tumor cells, which upregulates ADAM10 expression. ADAM10 in turn mediates the cleavage of CX3CL1 and activates the CX3CR1 receptor, inducing epithelial-mesenchymal transition (EMT) and RhoA signaling activation, thereby promoting tumor cell migration, invasion, and lung metastasis [53]. Recent studies have further shown that elevated platelet counts may predict worse prognosis in patients with advanced HCC [54]. In addition, PDW and MPV have also been demonstrated to be associated with HCC development, progression, and prognosis [55, 56]. Taken together, the mFI-5+PIS combined index is not a simple additive combination of several indicators. Rather, it concurrently encompasses systemic frailty, inflammation, cellular senescence, and the roles of platelets in tumor progression, metastasis, and treatment resistance. Such a combined index enables a more comprehensive assessment of prognostic risk after TACE in HCC patients from multiple perspectives.

The mFI-5 and PIS are based on routine medical history collection and routine blood testing. Both are easy to operate and can be easily integrated into the routine clinical workflow. For patients with high mFI-5 combined with PIS scores, more caution should be exercised when making initial treatment decisions for TACE. The clinical recommendation is to comprehensively evaluate the feasible systemic treatment plan or local-systemic combined treatment strategy, and avoid over-reliance on repeated TACE treatment to prevent liver failure. During the follow-up phase, monitoring and supportive treatment should be strengthened in order to detect early signs of disease progression or functional deterioration. In addition, mFI-5 combined with PIS scoring is expected to serve as a supplementary tool for existing staging systems such as BCLC and Albumin-Bilirubin Grading (ALBI), further refining the stratification of highly heterogeneous patients in the same stage. For example, for BCLC stage B patients with multiple tumors but no portal vein tumor thrombus (PVTT), those with low combined scores can still benefit from standardized TACE treatment, while high-risk patients with combined scores should consider combined treatment or converting to systemic treatment as soon as possible. This method can provide a more refined basis for optimizing the treatment strategy. In addition, the nomogram model constructed in this study demonstrated stable performance in external validation, further strengthening the credibility of this scoring tool for clinical promotion and application.

This study has a multicenter design, and the sample size is relatively large compared to other TACE-related studies; however, issues of selection bias and information bias may still exist. The majority of patients in our cohort had hepatitis B virus-associated HCC, and whether these findings are applicable to Western populations predominantly affected by alcoholic or metabolic dysfunction-associated steatotic liver disease warrants further validation through multicenter prospective studies. Moreover, this study did not incorporate molecular biomarkers or radiomic features. In the future, integrating mFI-5+PIS with imaging heterogeneity, genetic mutation profiles, and immune microenvironment characteristics may enable the construction of a more comprehensive multi-omics risk model, thereby better serving clinical prognostic assessment and treatment decision-making.

The present study found that an increased mFI-5+PIS score was significantly associated with a higher risk of overall mortality (HR = 1.8) and disease progression (HR = 2.2). Based on this continuous risk gradient, when formulating treatment strategies, clinicians should avoid repeated TACE in patients with an mFI-5+PIS score above the median of the cohort to prevent cumulative liver function impairment. For these patients, it is recommended to initiate combined targeted therapy or immunotherapy (systemic therapy) after the first TACE session, or to directly switch to systemic therapy. Furthermore, the follow-up interval should be dynamically adjusted according to the score; the higher the score, the shorter the interval between imaging examinations and AFP monitoring should be. In addition, for patients with a single mFI-5 component score of ≥ 2 (i.e., frailty), rehabilitation intervention and nutritional support should be implemented proactively, regardless of the PIS score. These suggestions fall within a risk-stratified management model, and future decision curve analysis may help determine specific intervention thresholds.

Conclusion

The mFI-5+PIS combined score constructed in this study is an independent and significant predictor of OS and PFS in HCC patients treated

with TACE. This tool can effectively predict the long-term survival outcome of patients.

Disclosure of conflict of interest

None.

Address correspondence to: Feng Guo, Department of Interventional Diagnosis and Treatment, Yongzhou Central Hospital, Yongzhou Clinical College, University of South China, No. 396 Yiyun Road, Lengshuitan District, Yongzhou 425000, Hunan, China. E-mail: search_gf@163.com; Xun Ma, Department of Oncology, Yongzhou Central Hospital, Yongzhou Clinical College, University of South China, No. 396 Yiyun Road, Lengshuitan District, Yongzhou 425000, Hunan, China. E-mail: hello_xun1988@163.com

References

[1] Vogel A, Meyer T, Sapisochin G, Salem R and Saborowski A. Hepatocellular carcinoma. Lancet 2022; 400: 1345-1362.

[2] Singal AG, Kanwal F and Llovet JM. Global trends in hepatocellular carcinoma epidemiology: implications for screening, prevention and therapy. Nat Rev Clin Oncol 2023; 20: 864-884.

[3] Akahoshi K, Shindoh J, Tanabe M, Ariizumi S, Eguchi S, Okamura Y, Kaibori M, Kubo S, Shimada M, Taketomi A, Takemura N, Nagano H, Nakamura M, Hasegawa K, Hatano E, Yoshizumi T, Endo I and Kokudo N. Oncological resectability criteria for hepatocellular carcinoma in the era of novel systemic therapies: The Japan Liver Cancer Association and Japanese Society of Hepato-Biliary-Pancreatic Surgery expert consensus statement 2023. Liver Cancer 2024; 13: 0-10.

[4] Kudo M, Ueshima K, Saeki I, Ishikawa T, Inaba Y, Morimoto N, Aikata H, Tanabe N, Wada Y, Kondo Y, Tsuda M, Nakao K, Ito T, Hosaka T, Kawamura Y, Kuzuya T, Nojiri S, Ogawa C, Koga H, Hino K, Ikeda M, Moriguchi M, Hisai T, Yoshimura K, Furuse J and Arai Y. A phase 2, prospective, multicenter, single-arm trial of transarterial chemoembolization therapy in combination strategy with lenvatinib in patients with unresectable intermediate-stage hepatocellular carcinoma: TACTICS-L trial. Liver Cancer 2023; 13: 99-112.

[5] An C, Wu S, Zuo M, Li W, Li K and Wu P. Surgical resection versus thermal ablation: comparison of sequential options after successful TACE downstaging therapy for unresectable hepatocellular carcinoma. Ther Adv Med Oncol 2025; 17: 17588359241306648.

[6] Yan HT, Zu QQ, Hua HJ, Fan WL, Cheng Y, Liu S, Shi HB, Feng ZL and Zhang JX. MRI-based quantification of intratumoral heterogeneity predicts response in hepatocellular carcinoma treated with atezolizumab-bevacizumab and TACE/HAIC. Acad Radiol 2025; 32: 6451-6462.

[7] Zheng X, Song X, Zhang B, Chen X, Zhang Y, Luo Q, Li Z, Deng Z, Xu R, Peng L and Xie C. Evaluating the impact of treatment sequencing on outcomes in hepatocellular carcinoma: a comparative analysis of TACE and systemic therapies. Clin Exp Med 2024; 24: 238.

[8] Lin HS, Watts JN, Peel NM and Hubbard RE. Frailty and post-operative outcomes in older surgical patients: a systematic review. BMC Geriatr 2016; 16: 157.

[9] Subramaniam S, Aalberg JJ, Soriano RP and Divino CM. New 5-factor modified frailty index Using American College of Surgeons NSQIP data. J Am Coll Surg 2018; 226: 173-181, e178.

[10] Shao YF, Zu YN, Yin XQ, Xiao JC and Gu YM. Impact of frailty on the long-term prognosis of the elderly with hepatocellular carcinoma treated with transarterial chemoembolization. Sci Rep 2025; 15: 12746.

[11] Tran A, Putnam LR, Lipham JC and Shiraga S. Utility of the mFI-5 as a predictor of post-operative outcomes following gastrectomy for gastric cancer: an ACS-NSQIP analysis. Surg Endosc 2024; 38: 5922-5928.

[12] Jimenez AE, Cicalese KV, Chakravarti S, Porras JL, Azad TD, Jackson CM, Gallia GL, Bettegowda C, Weingart J and Mukherjee D. Social determinants of health and the prediction of 90-day mortality among brain tumor patients. J Neurosurg 2022; 137: 1338-1346.

[13] Muhammed A, Fulgenzi CAM, Dharmapuri S, Pinter M, Balcar L, Scheiner B, Marron TU, Jun T, Saeed A, Hildebrand H, Muzaffar M, Navaid M, Naqash AR, Gampa A, Ozbek U, Lin JY, Perone Y, Vincenzi B, Silletta M, Pillai A, Wang Y, Khan U, Huang YH, Bettinger D, Abugabal YI, Kaseb A, Pressiani T, Personeni N, Rimassa L, Nishida N, Di Tommaso L, Kudo M, Vogel A, Mauri FA, Cortellini A, Sharma R, D'Alessio A, Ang C and Pinato DJ. The systemic inflammatory response identifies patients with adverse clinical outcome from immunotherapy in hepatocellular carcinoma. Cancers (Basel) 2021; 14: 186.

[14] Chen H, Wu Q, Zhang Y, Li Q, Ma J, Kong F and Ma X. Nomograms based on the novel platelet index score predict postoperative prognosis in endometrial cancer. Gynecol Oncol 2020; 158: 689-697.

[15] Kudo M, Ren Z, Guo Y, Han G, Lin H, Zheng J, Ogasawara S, Kim JH, Zhao H, Li C, Madoff DC, Ghobrial RM, Kawaoka T, Gerolami R, Ikeda M,

Kumada H, El-Khoueiry AB, Vogel A, Peng X, Mody K, Dutcus C, Dubrovsky L, Siegel AB, Finn RS and Llovet JM; LEAP-012 investigators. Transarterial chemoembolisation combined with lenvatinib plus pembrolizumab versus dual placebo for unresectable, non-metastatic hepatocellular carcinoma (LEAP-012): a multicentre, randomised, double-blind, phase 3 study. Lancet 2025; 405: 203-215.

[16] Fite EL and Makary MS. Transarterial chemoembolization treatment paradigms for hepatocellular carcinoma. Cancers (Basel) 2024; 16: 2430.

[17] Hatanaka T, Yata Y, Naganuma A and Kakizaki S. Treatment strategy for intermediate-stage hepatocellular carcinoma: transarterial chemoembolization, systemic therapy, and conversion therapy. Cancers (Basel) 2023; 15: 1798.

[18] Zhang Q, Wang Z, Song M, Liu T, Ding J, Deng L, Zhang X, Qian L, Ge Y, Xie H, Ruan G, Song C, Yao Q, Xu H, Ju H and Shi H. Effects of systemic inflammation and frailty on survival in elderly cancer patients: results from the INSCOC study. Front Immunol 2023; 14: 936904.

[19] Sumitomo R, Tsuji K, Katsuragawa H, Fukui T, Menju T, Kobayashi M, Sakai H and Date H. Pretreatment platelet level is associated with tumor proliferation and prognosis in malignant pleural mesothelioma. Gen Thorac Cardiovasc Surg 2025; 73: 784-792.

[20] Liu S, Fang J, Jiao D and Liu Z. Elevated platelet count predicts poor prognosis in breast cancer patients with supraclavicular lymph node metastasis. Cancer Manag Res 2020; 12: 6069-6075.

[21] Huang L, Li Z, Jian M, Wu X, Chen H, Qin H, Li Z, Song S, Xie Y and Chen R. Application of MFI-5 in severe complications and unfavorable outcomes after radical resection of colorectal cancer. World J Surg Oncol 2023; 21: 307.

[22] Khalid A, Pasha SA, Demyan L, Standring O, Newman E, King DA, DePeralta D, Gholami S, Weiss MJ and Melis M. Modified 5-Item Frailty Index (mFI-5) may predict postoperative outcomes after pancreatoduodenectomy for pancreatic cancer. Langenbecks Arch Surg 2024; 409: 286.

[23] Lee ACH, Lee SM and Ferguson MK. Frailty is associated with adverse postoperative outcomes after lung cancer resection. JTO Clin Res Rep 2022; 3: 100414.

[24] Torimura T and Iwamoto H. Optimizing the management of intermediate-stage hepatocellular carcinoma: current trends and prospects. Clin Mol Hepatol 2021; 27: 236-245.

[25] Waller KMJ, Prince DS, Lai EHY, Levy MT, Strasser SI, McCaughan GW, Teng MLP, Huang DQ and Liu K. The liver frailty index predicts survival in systemic therapy for hepatocellular carcinoma: a multicentre prospective cohort study. ESMO Gastrointest Oncol 2024; 3: 100043.

[26] Tandon P, Zanetto A, Piano S, Heimbach JK and Dasarathy S. Liver transplantation in the patient with physical frailty. J Hepatol 2023; 78: 1105-1117.

[27] Liu Y, Zhang Y, Ding Y and Zhuang R. Platelet-mediated tumor metastasis mechanism and the role of cell adhesion molecules. Crit Rev Oncol Hematol 2021; 167: 103502.

[28] Gan J, Zhang X and Guo J. The role of platelets in tumor immune evasion and metastasis: mechanisms and therapeutic implications. Cancer Cell Int 2025; 25: 258.

[29] Zvetkova E, Ivanov I, Koytchev E, Antonova N, Gluhcheva Y, Alexandrova-Watanabe A and Kostov G. Hematological and hemorheological parameters of blood platelets as biomarkers in diabetes mellitus type 2: a comprehensive review. Appl Sci (Basel) 2024; 14: 4684.

[30] Izzi B, Gialluisi A, Gianfagna F, Orlandi S, De Curtis A, Magnacca S, Costanzo S, Di Castelnuovo A, Donati MB, de Gaetano G, Hoylaerts MF, Cerletti C and Iacoviello L; On Behalf Of The Moli-Family Study Investigators. Platelet Distribution width is associated with P-selectin dependent platelet function: results from the Moli-family cohort study. Cells 2021; 10: 2737.

[31] Lin W, Wang H, Zhong M, Yu S, Zhao S, Liang S, Du J, Cheng B, Gu W and Ling C. Effect and molecular mechanisms of Jiedu recipe on hypoxia-induced angiogenesis after transcatheter arterial chemoembolization in hepatocellular carcinoma. Evid Based Complement Alternat Med 2021; 2021: 6529376.

[32] Rab SO, Altalbawy FMA, Bishoyi AK, Ballal S, Kareem M, Singh A, Kubaev A, Soleimani Samarkhazan H and Bagheri S. Targeting platelet-tumor cell interactions: a novel approach to cancer therapy. Med Oncol 2025; 42: 232.

[33] Strasenburg W, Jóźwicki J, Durślewicz J, Kuffel B, Kulczyk MP, Kowalewski A, Grzanka D, Drewa T and Adamowicz J. Tumor cell-induced platelet aggregation as an emerging therapeutic target for cancer therapy. Front Oncol 2022; 12: 909767.

[34] Schmied L, Höglund P and Meinke S. Platelet-mediated protection of cancer cells from immune surveillance - possible implications for cancer immunotherapy. Front Immunol 2021; 12: 640578.

[35] Sun Y, Li T, Ding L, Wang J, Chen C, Liu T, Liu Y, Li Q, Wang C, Huo R, Wang H, Tian T, Zhang C, Pan B, Zhou J, Fan J, Yang X, Yang W, Wang B and Guo W. Platelet-mediated circulating tumor cell evasion from natural killer cell killing

through immune checkpoint CD155-TIGIT. Hepatology 2025; 81: 791-807.
[36] Sepúlveda M, Arauna D, García F, Albala C, Palomo I and Fuentes E. Frailty in aging and the search for the optimal biomarker: a review. Biomedicines 2022; 10: 1426.
[37] Pan Y and Ma L. Inflammatory markers and physical frailty: towards clinical application. Immun Ageing 2024; 21: 4.
[38] Saglam Oz M, Toprak B, Bora R and Demir I. The role of hematological parameters in critically ill patients: mortality prediction in elderly intensive care unit patients. Cureus 2025; 17: e82183.
[39] Cognasse F, Duchez AC, Audoux E, Ebermeyer T, Arthaud CA, Prier A, Eyraud MA, Mismetti P, Garraud O, Bertoletti L and Hamzeh-Cognasse H. Platelets as key factors in inflammation: focus on CD40L/CD40. Front Immunol 2022; 13: 825892.
[40] Scherlinger M, Richez C, Tsokos GC, Boilard E and Blanco P. The role of platelets in immune-mediated inflammatory diseases. Nat Rev Immunol 2023; 23: 495-510.
[41] Chen D, Li Y, Liu L, You N, Wang L, Wang Z, Zheng L and Li J. Association of 5-factor modified frailty index and controlling nutritional status score with overall survival in patients with unresectable hepatocellular carcinoma undergoing interventional therapy. J Army Med Univ 2025; 47: 2061-2070.
[42] Zhu HL, Cai CY, Li BY, Tang CQ, Ren YN and Li DY. Construction of a nomogram for predicting postoperative recurrence of hepatocellular carcinoma patients based on the novel platelet index score. J Abdom Surg 2025; 38: 229-238.
[43] Lema-Arranz C, Hemadeh A, Fernández-Bertólez N, Cibeira N, López-López R, Costa S, Millán-Calenti JC, Lorenzo-López L, Valdiglesias V and Laffon B. Association of inflammatory biomarkers with physical and cognitive frailty in a Spanish population of older adults. GeroScience 2026; 48: 2063-2084.
[44] Yoon JK and Choi JY. MRI imaging biomarkers for prognostication of hepatocellular carcinoma. J Korean Soc Radiol 2025; 86: 364-380.
[45] Li L, Li Z, Zhang Y, Zhu S, Ni Y, Xu L, Yan S and Tang Y. Liver resection versus targeted therapy plus PD-1 inhibitors in hepatocellular carcinoma with type I-II portal vein tumor thrombus: a comparative study. J Hepatocell Carcinoma 2025; 12: 2745-2754.
[46] Donghia R, Carr BI and Yilmaz S. Factors relating to tumor size and survival in patients with hepatocellular carcinoma: significance of platelet-lymphocyte ratio, portal vein thrombosis, and albumin. Oncology 2026; 104: 145-155.
[47] Perisetti A, Goyal H, Yendala R, Chandan S, Tharian B and Thandassery RB. Sarcopenia in hepatocellular carcinoma: current knowledge and future directions. World J Gastroenterol 2022; 28: 432-448.
[48] VanHook AM. Bypassing senescence. Sci Signal 2025; 18: eadv9441.
[49] Ramaite FT and Nkadimeng SM. Targeting inflammatory pathways in hepatocellular carcinoma: recent developments. Discov Oncol 2025; 16: 1174.
[50] Wu C, Dong J, Sui S, Tan X and Zhu N. Inflammation in hepatocellular carcinoma progression: a “Single Wick, dual interwoven strands” regulatory framework. Front Immunol 2026; 17: 1822039.
[51] Anton A, Friedman SL and Cogliati B. Hepatic fibrosis and liver cancer. Semin Liver Dis 2026; 46: 31-50.
[52] Pavlović N, Kopsida M, Gerwins P and Heindryckx F. Activated platelets contribute to the progression of hepatocellular carcinoma by altering the tumor environment. Life Sci 2021; 277: 119612.
[53] Gao JH, He AD, Liu LM, Zhou YJ, Guo YW, Lu M, Zeng XB, Gong X, Lu YJ, Liang HF, Zhang BX, Ma R, Zhang RY and Ming ZY. Direct interaction of platelet with tumor cell aggravates hepatocellular carcinoma metastasis by activating TLR4/ADAM10/CX3CL1 axis. Cancer Lett 2024; 585: 216674.
[54] Munker S, Rodriguez I, Bernhart K, Ben Khaled N, Findik M, Siegmund LK, Ye L, Reiter FP, Roessler D, Nasseh D, Balcar L, Pomej K, Scheiner B, Weiss C, Pinter M, Seidensticker M, Mayerle J, Philipp AB and De Toni EN. Prognostic significance of elevated platelet count (> 200 x 10^9 per L) in BCLC stages B and C of hepatocellular carcinoma: a retrospective multicenter analysis. J Hepatocell Carcinoma 2025; 12: 855-864.
[55] Guo F, Zhu X and Qin X. Platelet distribution width in hepatocellular carcinoma. Med Sci Monit 2018; 24: 2518-2523.
[56] Şentürk M, İnce V, Üreyen O, Eyvaz K, Işık B, Carr BI and Yılmaz S. Mean platelet volume is a poor prognostic factor in patients undergoing liver transplantation for hepatocellular carcinoma. Turk J Gastroenterol 2025; 36: 169-173.